BRNO UNIVERSITY OF TECHNOLOGY
VYSOKÉ UČENÍ TECHNICKÉ V BRNĚ

FACULTY OF INFORMATION TECHNOLOGY
FAKULTA INFORMAČNÍCH TECHNOLOGIÍ

DEPARTMENT OF INTELLIGENT SYSTEMS
ÚSTAV INTELIGENTNÍCH SYSTÉMŮ

CREATING A DEPTH MAP OF EYE IRIS IN VISIBLE SPECTRUM

VYTVOŘENÍ HLOUBKOVÉ MAPY OČNÍ DUHOVKY VE VIDITELNÉM SVĚTLE

MASTER'S THESIS
DIPLOMOVÁ PRÁCE

AUTHOR **Bc. MARTIN KUBÍČEK**
AUTOR PRÁCE

SUPERVISOR **prof. Ing., Dipl.-Ing. MARTIN DRAHANSKÝ, Ph.D.**
VEDOUCÍ PRÁCE

BRNO 2019

Brno University of Technology
Faculty of Information Technology

Department of Intelligent Systems (DITS) Academic year 2018/2019

Master's Thesis Specification

Student: **Kubíček Martin, Bc.**

Programme: Information Technology Field of study: Intelligent Systems

Title: **Creating a Depth Map of Eye Iris in Visible Spectrum**

Category: Signal Processing

Assignment:

1. Study the literature about iris imaging, especially using natural light (visible spectrum).
2. Design an optic illumination for eye iris with a low stress and very high comfort for the iris or use an existing solution.
3. Collect a database with eye irises in high resolution and sharpness, if possible including veins and arteries in sclera, with minimally 100 samples.
4. Select and implement the most sufficient macro stacking method and create the resulting image with the best depth of field.
5. Compare the created images with existing technology and evaluate their benefits or suggest further improvements.
6. Based on the achieved results create a methodology for iris scanning.

Recommended literature:

- Zhang D., Guo Z., Gong Y. *Multispectral Iris Acquisition System*. Multispectral Biometrics, Springer, 2016, pp. 39-62, ISBN 978-3-319-22485-5.
- Trigg G.L. *Encyclopedia of Applied Physics*. Wiley, Vol. 23, p. 628, ISBN 978-3527294763.

Detailed formal requirements can be found at http://www.fit.vutbr.cz/info/szz/

Supervisor: **Drahanský Martin, prof. Ing., Dipl.-Ing., Ph.D.**

Head of Department: Hanáček Petr, doc. Dr. Ing.

Beginning of work: July 1, 2019

Submission deadline: July 31, 2019

Approval date: July 26, 2019

Abstract

The aim of the master thesis is to propose and introduce in practice the methodology of scanning the iris of an eye in the visible spectrum. It emphasizes the quality of images, credible color rendering in comparison to the real basis and, in particular, the continuous depth of sharpness that could reveal previously unexamined aspects and details of the iris. Last but not least, the thesis will also focus on minimizing exposure to physical stress tot he iris. Part of the methodology is a precise procedure for iris imaging while ensuring image consistency. This will allow the creation of an iris database that tracks their evolution in time or other aspects such as the psychological state of the person being scanned. To start with in practice, the anatomy of the human eye and especially that of the iris is presented. Known methods of iris scanning are given. Then, there is a section about proper iris lighting. This is necessary for the desired level of image quality but at the same time it exposes the eye to great physical stress. It is therefore necessary to find a compromise between these factors. Important is the very description of the methodology itself as it describes in detail the scan. Furthermore, the thesis deals with necessary post-production adjustments, such as compiling images with different depths of sharpness into a single continuous image or applying filters to remove defects from the images. The last part of the thesis is divided into evaluation of the results and the conclusion in which is discussed the possible extension or modification of the methodology so that it can be used outside the laboratory conditions.

Abstrakt

Diplomová práce si dává za cíl navrhnout a uvést v praxi metodiku snímání oční duhovky ve viditelném spektru. Klade přitom důraz na kvalitu snímků, věrohodné podání barev vůči reálnému podkladu a hlavně na kontinuální hloubku ostrosti, která odhaluje dosud nezkoumané aspekty a detaily duhovky. V poslední řadě se také soustředí na co nejmenší vystavení duhovky fyzickému stresu. Metodika obsahuje přesné postupy jak snímat duhovku a zajišťuje tím konzistentnost snímků. Tím umožní vytvářet databáze duhovek s ohledem na jejich vývoj v čase či jiném aspektu jako je například psychologický stav snímané osoby. Na úvod je v práci představena anatomie lidského oka a zejména pak duhovky. Dále pak známé způsoby snímání duhovky. Následuje část, jež se zabývá správným osvětlením duhovky. To je nutné pro požadovanou úroveň kvality snímků zároveň ale vystavuje oko velkému fyzickému stresu. Je tedy nutné najít kompromis mezi těmito aspekty. Důležitý je popis samotné metodiky obsahující podrobný popis snímání. Dále se práce zabývá nutnými postprodukčními úpravami jako je například složení snímků s různou hloubkou ostrosti do jednoho kontinuálního snímku či aplikací filtrů pro odstranění vad na snímcích. Poslední část práce je rozdělena na zhodnocení výsledků a závěr, v němž se rozebírají možné rozšíření či úpravy metodiky tak, aby ji bylo možné použít i mimo laboratorní podmínky.

Keywords

iris, scanning, visible spectrum, bepth map, depth of field

Klíčová slova

duhovka, snímaní, viditelné světlo, hloubková mapa, hloubka ostrosti

Reference

KUBÍČEK, Martin. *Creating a Depth Map of Eye Iris in Visible Spectrum.* Brno, 2019. Master's thesis. Brno University of Technology, Faculty of Information Technology. Supervisor prof. Ing., Dipl.-Ing. Martin Drahanský, Ph.D.

Rozšířený abstrakt

V dnešní době, kdy jsou otázky bezpečnosti stále více zmiňovány, a to i laickou veřejností, je potřeba tyto vědní obory rozvíjet a posouvat dále. Zejména pak biometrii, jenž pracuje s unikátními vlastnostmi člověka, které nelze jednoduše ztratit, zapomenout, či si nechat odcizit. Avšak s rostoucím vývojem moderní techniky, není poslední jmenované takový problém. Proto je potřeba přicházet se stále novými metodami, jak získávat lepší a přesnější biometrické data. Ať už díky kombinaci jednotlivých biometrických dat a vytvoření multimodálních biometrických systémů, tak díky zvyšování kvalitativních nároků na jednotlivé biometriky či hledání úplně nových jako je tomu například u DNA.

Většina výzkumníků tedy cílí na zlepšování kvality výsledných dat. To sebou však často přináší velmi zdlouhavé a mnohdy náročné snímání. Protipólem jsou výrobci biometrických zařízení a běžní uživatelé, kteří takovému zdlouhavému snímání nechtějí být podrobeni. Cílí především na rychlost a pohodlnost při snímání, než na kvalitu a přesnost. Určitou roli zde hraje i marketingový faktor, v němž někteří výrobci slibují použití nejmodernějších metod a technologií, přičemž opak je pravdou či jsou použité metody značně okleštěné, právě z důvodu většího pohodlí pro uživatele. Je tedy čím dál větší výzvou mezi těmito skupinami najít společný průnik.

Těmi nejčastěji zmiňovanými metodami jsou: 3D/2D sken obličeje, otisk prstu, snímání sítnice, případně duhovky. Duhovka společně se sítnicí jsou nejméně skloňované a to z důvodu, že k jejich snímání je potřeba speciálního hardwaru. Proto se těmito biometrickými daty zabýváme spíše v rámci rozvoje pro medicínské účely.

Tyto faktory byli hlavní motivací pro počáteční zkoumání a následné vyvíjení metodiky, jenž bude využívat dostupnější hardware a generovat výsledky v odpovídající kvalitě. Tato práce popisuje zkoumání metodiky snímání lidské duhovky ve viditelném světle za použití běžně dostupných fotoaparátů a příslušného vybavení. Dává si také za cíl eliminovat stresové faktory, kterým jsou snímaní lidé vystaveni. Jednak psychické, ze strachu z obrovských přístrojů, jenž se používají u oftalmologů a druhak výraznému snížení fyzického stresu, kterému je snímané oko podrobeno, ve chvíli kdy je potřeba správně osvětlit duhovku. V poslední řadě pak práce cíli na kvalitu vyprodukovaných snímků, jenž budou následně sloužit pro další zpracování.

V kapitole 2 je obecně popsaná anatomie lidského oka a především duhovky. A to hlavně z důvodu, že je potřeba vědět, jak celý oční systém funguje, znát jeho specifika a detaily na které je možné se při tvorbě metodiky zaměřit. Dále lze v kapitole 3 nalézt popis stávajících metod snímání oční duhovky, kterému v dnešní době stále vévodí snímání v infračerveném spektru, ale také pomalu rozvíjející se snímání ve viditelném spektru. Pro snímání ve viditelném spektru je poté klíčové speciální zdroj světla, to udává míru detailu, ale také vystavuje snímané oko určité míře stresu. Těmito aspekty a hlavně návrhem vlastního řešení se zabírá kapitola 4. V kapitole 5 je popsána výsledná metodika, jenž byla vytvořena postupným iterováním teoretických znalostí a experimentováním. Obsahuje také poznatky, které při postupném vyvíjení metodiky vznikli z experimentálního testování. Na výsledné snímky vzniknuté z metodiky, byly aplikovány nejrůznější postprodukční metody. Zejména metody zabývající se skládáním makro snímků s cílem dosáhnout, co nejlepší možné kvality snímků. Dále také rozličné obrazové filtry pro zvýraznění hloubkové mapy duhovky. Popsané výsledky lze najít v kapitole 6. V poslední řadě bylo důležité zhodnocení dosáhnutých výsledků a porovnání s existujícími řešeními. Především z pohledu kvality hloubkové mapy, úrovně stresového faktoru pro lidské oko a celkového pohledu na metodiky a použité technologie. Zmíněny jsou také jevy, které bylo možné pozorovat během snímání a vykazovaly podobné rysy, mezi většinou snímaných.

Díky metodice tak vznikla unikátní databáze očních duhovek ve vysoké kvalitě, jenž bude dále podrobená zkoumání v rámci výzkumné skupiny STRaDe a také bude poskytnuta oftalmologům ze zkoumání pozorovaných jevů během snímání. Databáze se bude nadále rozvíjet a s ní také metodika, jejíž možné další vylepšení jsou zmíněné v rámci práce a došlo k nim zejména zpětným analyzováním výsledků.

Creating a Depth Map of Eye Iris in Visible Spectrum

Declaration

I declare that I have prepared this Master's thesis independently under the supervision of prof. Ing., Dipl.-Ing. Martin Drahanský, Ph.D. Further information was provided by MUDr. Tomáš Mňuk. I have listed all of the literary sources and publications that I have used.

.....
Martin Kubíček
July 31, 2019

Acknowledgements

I would like to thank prof. Ing., Dipl.-Ing. Martin Drahanský for supervising this work and for providing a lot of valuable advice that contributed to this work. Furthermore, I would like to thank MUDr. Tomáš Mňuk, for providing professional materials and advice on ophthalmology.

Contents

Chapter 1

Introduction

The aim of this work is to design and develop a methodology, thanks to which it would be possible to create a stacked macro photograph of the iris of the eye in the visible light spectrum. A photo thus created, which consists of multiple photographs with different depth of field, is used to create a model. This methodology is carried out in the colour spectrum, and thus the resulting model contains information about the colour of the iris.

Nowadays, with the issue of security being of utmost interest and with the greater use of biometrics for safeguarding, there is the need to find and explore better and newer methods of imaging and preserving biometric data, for example by combining them (multi-modal biometric system). For example, connecting fingerprints and blood vessel patterns or improvements to the imaging, and thus obtaining better quality biometric data for comparison. This necessity also arises thanks to modern technology, the development of which has seen great advances and, at the moment, allows us to make sensors so small that they can easily fit into a mobile phone or into other smart devices. The quality of the sensors themselves has improved as well as the data generated by them, however, this also means an increase in the difficulty of their verification. Finally yet importantly, is the fact that these technologies today are much more accessible and it is possible to carry out their reverse engineering or get the required biometric data. This then contributes to the emergence of increasingly better methods, how to bypass current biometric systems, for example, using a fake lens with a printed iris or an artificially generated fingerprint.

The main motivation to create this methodology is, first, that it would create a database of high-quality images of the iris of the eye, which will be of importance, both for further use in bio-criteria and for use in medicine or in any other field of science. The created methodology will then include accurate and constant conditions for how images are made. Subsequently, it will be possible to observe in time the development of individual irises and, thanks to this, observe pathological factors of the iris. An important factor in the methodology is the very imaging in the visible light spectrum, which adds an aspect that allows checking even the colour of the iris, changes or possible development over a period, of which could be beneficial especially in the field of medicine, where this situation has only partially been solved. Another aspect, to which colour contributes is a new level of safety and the robustness of biometric systems, current systems do not take into account the colour of the iris and rather combine this technology with other elements of biometrics, creating more demanding multi-modal biometric systems that are not very convenient for the imaged object. Thus, the aim is to exploit the potential that the colour of the iris offers to create a robust system without the need to image more biometric data.

In this work, the anatomy of the human body is generally described in Chapter 2, and mainly, the anatomy of the iris. Chapter 3 further describes the methods of imaging the iris of the eye, mainly subsequent imaging in the infrared and visible spectrum. First of all, then the necessary equipment for imaging problems of various methods, and more concretely, their results. Chapter 4 then, in detail focuses on imaging in the visible light spectrum, especially on the biggest problem, namely lighting and the proposal. Chapter 5 follows by describing the methodology of imaging itself and the components used. Chapter 6 then covers the creation of stacked macro photographs, applying filters and creating the resulting images. Chapter 7 contains an assessment of the results and a comparison with images obtained using the IR method. The conclusion and plans for possible expansion or improvement of the methodology can be found in Chapter 8.

Chapter 2

The Human Eye

The human eye is one of the most important paired organs in our body. It provides one of the basic human forms of perception, in this case, is sight, which serves to orient and perceive space or to discern colours. The eye is made up of the eyeball and other associated organs, which are the oculomotor muscles. Thanks to these six muscles, more precisely four lateral and two oblique muscles, the eye is the most mobile organ of the human body. The eyeball has the shape of an asymmetrical ball with a diameter of about 25mm and is located in the eye socket.[12]

The three basic structures of the eye are the cornea, the lens and the vitreous body, which are designed to be flexible and concentrate incoming rays of light so that they fall into the place of the sharpest vision that is on the retina. These rays creating an image on the retina are greatly reduced and, most importantly, inverted as opposed to the actual subject. Light rays hitting the retina trigger chemical transformations in photosensitive cells.[21] We divide these cells into rods, that serve to perceive the intensity of light, and cones, that are colour vision receptors. Subsequently, the cones are divided according to their pigmentation into red, green and blue.

In general, the basic parts of the human eye and its functionality can be described this way. Subsequently, in this chapter, we will analyse it more from the anatomical point of view and then focus primarily on the iris and on its structure. From this information can then be deduced, what data should be imaged and what information can be extracted from it.

2.1 Anatomy of the eye

A sagittal incision of the human eye (figure 2.1), respectively, of the eyeball, reveals a wall that consists of three tissue layers:

- **The outer layer** or sclera, is a thick, opaque, ligamentous membrane on the surface of the eyeball. It forms the solid envelope of the eyeball, which, in the anterior part of the surface, changes into a transparent cornea.
- **The middle layer** called the choroid, also envelops the entire eyeball and is located between sclera and retina. It is very rich in capillaries and contains cells with brown pigment. These prevent light rays scattering inside the eye. The front is formed by a ciliated body and the Iris. In the posterior part, it is then connected to the edges of the optic nerve.
- **The inner part** formed by the retina.

The eye also consists of two chambers in which aqueous humour, a derivative of blood plasma, circulates. The chambers are as follows:

- **The anterior chamber:** a slotted space located between the cornea and the anterior part of the iris.
- **The posterior chamber:** a slotted space located between the posterior part of the iris and the anterior part of the lens.

The remaining inner spaces of the eyeball are filled with the vitreous body, a transparent, jelly-like mass.

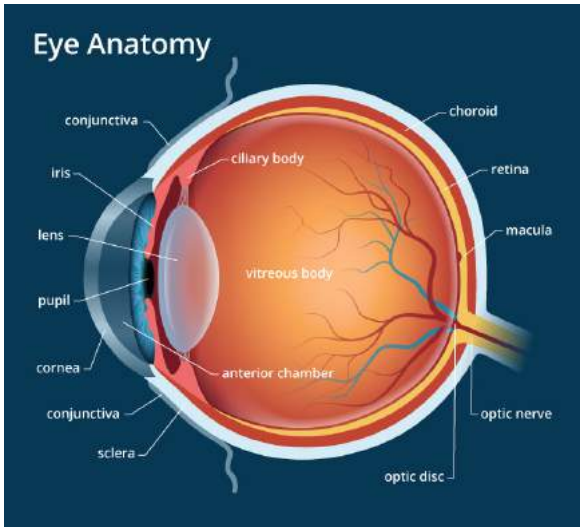

Figure 2.1: vertical cut of the human eye (taken from [26])

A detailed description of the individual functional parts of the eyeball as depicted by a sagittal cut in Figure 2.1:

- **The cornea**(*lat. cornea*), domed-shaped, clear tissue, located in the anterior part of the eyeball. One of the most sensitive parts of the human body, thanks to a large number of nerve endings, but it is not permeated with blood vessels, which gives it its transparency. Due to extreme sensitivity, it is prone to irritation, which leads to lacrimation and squinting. It affects the direction the rays of light are spread and is, therefore, the most important refractive of the eye. The cornea optical strength ranges from 40- 43D, which roughly represents 2/3 of the total optical strength of the eye.[21]

- **The iris**(*lat. iris*), is a smooth, circular muscle with a circular opening in the middle. By its stretching or shrinking, the size of the opening (pupil) changes. This mechanism serves to regulate the amount of light that penetrates into the interior; it thus acts as an aperture. More of which will be in the following sub-chapter 2.2.

- **The pupil**(*lat. pupilla*) is a circular opening in the centre of the iris of the eye. The pupillary light reflex, that is, how much it contracts or dilates, is determined by two groups of muscles: the iris sphincter muscle and the iris dilator muscle. These regulate the amount of light coming into the eye. The lens can be found behind the pupil.

- **The lens**(*lat. lens crystallina*) is a 4mm non-homogeneous biconvex bulging connecting body with a posterior surface that is more curved. The body is made of a rigid jelly-like and perfectly transparent mass. It hangs on the ciliary body with the help of the fibres known as the zonula of Zinn.[24] Its main function is the refraction of light, so that all incoming rays of light converge to one point on the retina, which is achieved by means of accommodation, changes in the dioptre strength of the eye with the help of the arching of the anterior surface of the lens. Accommodation depends on the distance of the object from the eye and allows you to focus on a given object. The optical strength of such a lens is then in the range of 15-20D.

- **The ciliary body**(*lat. corpus ciliare*), radially arranged muscle made up of smooth muscle fibre. The lens hangs on this muscle with the help of thin fibres. The body contributes significantly to lens accommodation, thanks to contractions of its musculature. This changes the curvature of the lens, thereby modifying its optical strength. From the blood that flows through the capillaries of the body intraocular fluid, called ventricular water, is produced. The latter then nourishes without the need vascular tissue of the eye, more precisely the cornea and lens, thereby maintaining the shape of the eye.

- **The vitreous body**(*lat. corpus vitreum*) is a clear gel-like tissue that fills the inner space of the eyeball, more precisely, between the lens and the retina. It serves to maintain the internal pressure of the eyeball and helps to keep of the spherical shape of the eyeball.

- **The macula**(*lat. macula lutea*), a round area with the greatest density of cones located in the visual axis of the eye. It is, therefore, the point of sharpest vision. This specific area located on the retina is yellowish-green in colour, which gives it its common name, **the Yellow Spot**.

- **The retina**(*lat. retina*), a thin multi-layered membrane that forms the inner wall of the human eye, the thickness of this membrane ranges from 0.2 mm to 0.4 mm.[12] On which the sensory cells are located. The cells are then divided into rods, which are sensitive to the intensity of light and thus serve to its perception, especially the perception of the level of detail (for example, light without colour information - black and white). Cones, on the contrary, are receptors of colour vision. These are further divided according to their pigment and sensitivity to wavelength, to red, green and blue. There is also a blind spot on the retina, which is the point where the optic nerve enters the eyeball. There are no light-sensitive cells at this point, so there are neither rods nor cones and because of this, the retina does not perceive images at this point. The macula, which is the point of sharpest vision, can be found near the blind spot.

- **The optic nerve**(*lat. nervus opticus*) is the convergence point in the blind spot into which they all neuronal fibres of ganglion cells penetrate the wall of the eyeball.[24] In this way, the optic nerve, which is a paired sensory cerebral nerve, is created. It transmits visual information from the retina to the visual centres.

- **Choroid**(*lat. choroidea*), a brown pigment layer enveloping the eyeball that is located between the sclera and the retina. In the anterior part, it passes into the ciliary body, and in the posterior part, it connects to the edges of the optic nerve. The choroid is densely permeated with blood capillaries; these then nourish the deep layers of the retina. It also prevents the scattering of light rays inside the eyeball.

- **The sclera**(*lat. sclera*) is a white, rigid and opaque, ligamentous membrane on the outer surface of the eye. In the front part of the eye, it passes into the cornea, and the optic nerve comes out of it in the back. The oculomotor muscles are also attached to it. The thickness of this membrane ranges from 0.3 mm to 1mm.[8]

2.2 Anatomy of the iris

A significantly pigmented spur of the choroid is located frontally between the lens and the eye sclera, thus also separating the anterior and posterior ocular ventricles. Thanks to pigmentation, it prevents the passage of light into the inner part of the eye other than through the pupil. The surface is irregular with a large number of stacks and grooves. Its average size is approximately 12mm; the width depends on the current size of the pupil.[21]

The functioning of the iris is very similar to the principle of the aperture at the photographic lens, this being the regulating the level of light entering the eye. The iris is associated with the delicate muscles that dilate the pupil when there is not enough light or contracts the pupil when there is sufficient or stronger light.[32] Such regulation is called accommodation of the pupil and it cannot be influenced at will, it happens spontaneously. The dilating muscle lies transversely to the border of the iris, which is attached to the muscle along the border of the iris. By contracting and dilating, the iris creates visible circular lines or grooves on its surface. In addition to these formations, white lines formed by the blood capillaries of the iris can be observed. The pupil can contract to a minimum diameter of 1.5 mm and dilate maximally up to a diameter of 8mm. Besides light conditions, the pupils can also respond to psychological or chemical signals.[7]

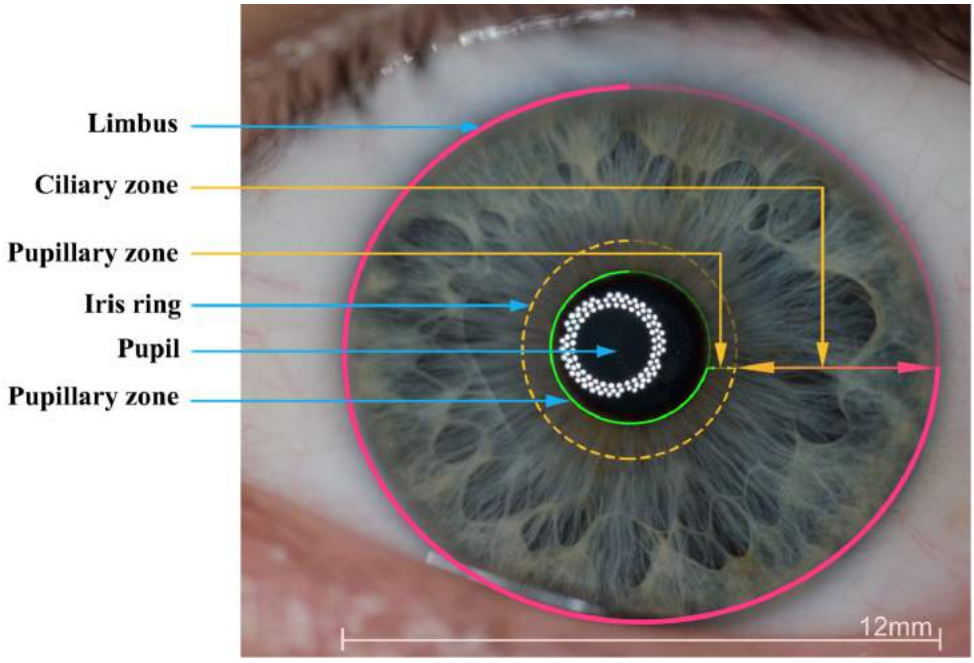

Figure 2.2: Detailed frontal image of the iris

2.2.1 The basic components

- **The limbus**(*lat. limbus corneae*) is the lateral area of the border transition between the sclera and the lens. It can also be considered the border with the iris. It is the thinnest part of the iris 0.5 mm, and sometimes it is referred to as the root of the iris.
- **The iris collarette**(*lat. collarette*) is a developed area located on average 1.5 - 2mm from the pupillary edge that divides the iris into two distinct, large parts: **the ciliary part** and **the pupillary part**. It has the shape of a wavy circle and is the widest part of the iris (0.6 - 1mm).
- **The ciliary zone**(*lat. zona ciliaris*) extends from the root of the iris (**Limbus**) to the iris mesentery. The width of the area is 3-4mm, and therefore it is the largest area of the iris. It is further divided into three parts. The first one closest to the mesentery is relatively smooth and features the appearance of rays-like furrows. Then, in the middle part, there are circular contraction furrows. The peripheral part is then characterized by the numerous appearance of crypts.
- **The pupillary zone**(*lat. zona pupillaris*) a relatively flat area that runs from the pupillary edge to the iris mesentery. In proportion to the ciliary zone, it is smaller, with a width of 1 - 2mm. There are not as many furrows on it as on the ciliary zone.
- **The pupil**(*lat. pupilla*) is a hole through which the sunlight passes into the eye. It is located roughly in the middle of the iris; however, its position is not exactly central. The size of the pupil under normal conditions is 3 - 4mm.

- **The pupillary margin**(*lat. margo pupillaris iridis*) is a thin hem bordering the pupillary zone and pupil. A dark edge can be observed on it, which rises to the foreground. This pigmented part protrudes from the back of the iris and makes the pupil look dark. Sometimes, this is called *the pupillary ruff*.

2.2.2 Features

The distinctive features of the iris develop in the first eighteen months of life, then the texture and features of the iris remain unchanged (except for colour). Significant changes then only occur with diseases or injuries of the iris. The anterior stroma cornea (*lat. substantia propria*) is formed by elastic and collagen fibres, the latter are then interwoven with smooth muscle. The posterior stroma is formed by a deeply pigmented two-layer tissue.

The combination of features, colour and texture are characteristic for every iris, and this applies even to the irises of the same person. The individual colours of the irises can then differ from each other (more in sub chapter 2.2.4). This creates more than 400 unique markers, which are used in bio-criteria, in particular for identification and verification.

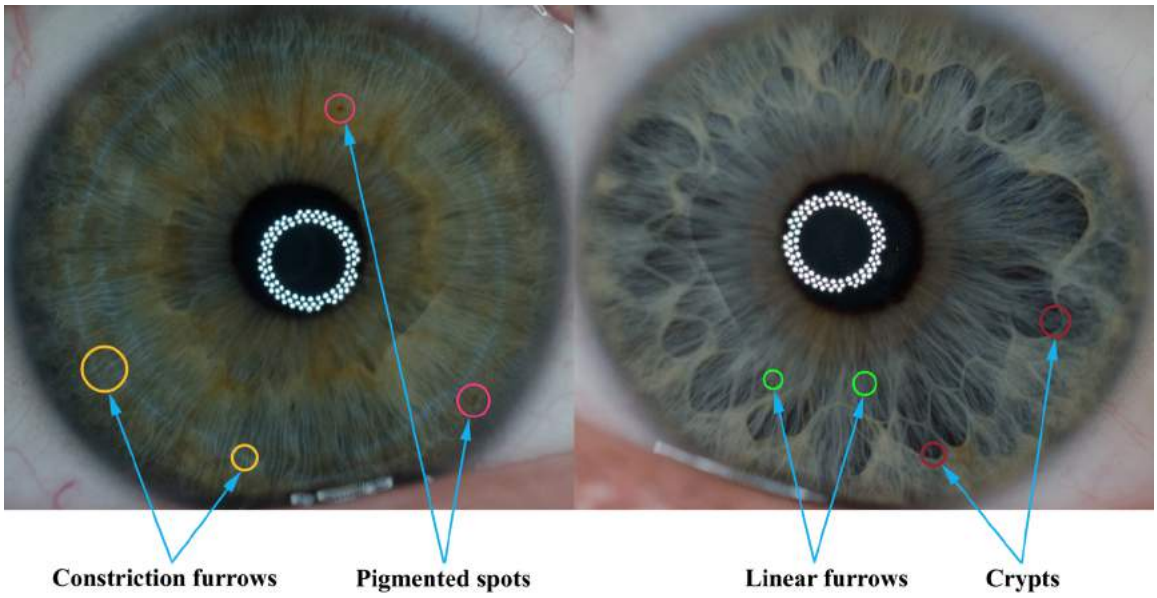

Figure 2.3: Sample of typical shapes in the iris of the eye

The texture then creates a couple of basic shapes, among the most significant and best visible, are **Crypts**. These are formed by sparse ligament, in which there are numerous pigment cells, smooth muscle cells and a network of blood vessels.[27] Most often, they have a circular, depressed form. The crypts that are located near the iris ring are then called Fuchs. Then, there are **pigmented spots**(*pigment spots*). These can be found anywhere on the iris except the pupils. These are small brown spots of irregular shape. **Furrows** are narrow, light formations. They are divided into two basic types, namely linear, which most often occur in the pupillary part, and the contraction furrows, in which movement can be observed when the pupil dilates. Contraction furrows are found predominantly in the ciliary part of the iris. Small, regular spots of white or grey colour that form a circle in the stroma of the iris around its perimeter, are called **the Wolfflin nodes**. Finally, various arched ligaments can also be found, rings, coronas, and ridges.

2.2.3 Colour

The colour of the iris is one of its most pronounced properties. This depends primarily on the thickness of the ligament stroma, the density, the filling of the blood vessels and the pigment, which shines through from the posterior part of the iris. It is produced by pigment cells, or **melanocytes**, which can also be found in the stroma of the iris. Although there is a nearly inexhaustible range of colour combinations of Iris, the pigment cell produces only one pigment. This is a dark colour known as melanin. There are two forms of melanin: **eumelanine**(*brown-black*), which is primarily responsible for the dark colour of the iris and for protection against UV rays, and **pheomelanine**(*yellow-red*), which occurs in the iris only to a very small extent or not at all and causes, for example the yellowish fragments of the iris.[19]

The exact colour and, most importantly, its intensity is influenced by many other factors. For example, the number of pigment cells in the iris, the latter greatly affects the saturation of colour or the content of red components in the blood circulating through the ophthalmic organ, which, to a small extent, affects the colour. Thus, the range of colours varies from light blue, through green-blue, or green, or varying degrees of grey to light brown, which then gradually passes on to deep, dark shades. Such eyes then are said to be black eyes.[33] The iris acquires shades of blue if there are few pigment cells. The light reflected from the back pigment layer then has a blue colour. If the pigment is also found in the stoma, green or brown shades are obtained. These also depend on the intensity of the pigment that the melanocytes produce.

Among other things, **the OC2 gene**, located on the 15^{th} *chromosome*, is responsible for colour.A second gene, **GEY** or **EYCL1** can be found on the 19^{th} *chromosome* in the green or blue variation, the latter also contributes greatly to the colouring of the eyes.[18]

The colour stabilizes during the first 3 years of life. New-borns tend to have a light blue to light purplish eye colour. This later fades away during the first year of life, mainly darkening. From the 3^{rd} year of life, there are changes that are more significant. However, the colour is not constant and oscillates around its base. Mainly due to hormones, which largely affect the formation of pigments in the body. In addition, the state of health or stress can also affect the production of pigmentation to some degree. The exact mechanism of how these changes work in the production of melanin, and therefore changes of colour is currently still not entirely known.

Figure 2.4: An overview of the basic colours of the iris. *Top left:* blue; *top right:* blue-green; *bottom left:* green-brown; *bottom centre:* light brown; *bottom right:* dark brown; (taken from [2])

2.2.4 Diseases

Multi-colouring of the iris is called **heterochromia**. This is caused by a lack of or excess of melanin production and either affects a part of the iris (*Heterochromia iridis*) or the whole iris (*Heterochromia iridium*). In complete heterochromia, a colour difference can be seen between the one iris and the other. In the partial form, two types are recognised: **central** and **sectoral**. The most common form of heterochromia is central and this is observed as a differently-colour circle, which most often occurs around the centre of the iris. While the sectoral form can be described as a non-specifically shaped segment, which differs in colour from the rest of the iris.

Heterochromia can be congenital, that is, genetic in origin, or arise because of disease of the iris or from injury. This is not a physiological phenomenon and it does not require a medical diagnosis. It does not directly threaten health. It is very rare and occurs only in a small percentage of the human population. There is no evidence of a link between the occurrence of heterochromia and gender.[33]

Figure 2.5: An example of heterochromia. *Top:* complete; *right:* central; *left:* sectoral

Albinism is a rare genetic disorder that stops the formation of the melanin pigment. (*Albinismus ocularis*), especially affecting only the eye. Lack of pigmentation is seen not only in the iris but also in the ciliary body or in the retina. The missing pigmentation in the iris then causes the iris to have a pink colour. This is because the missing pigment does not absorb colour rays, and therefore it is not coloured. Thus, the pink colour is formed by the shining of the red colour from the choroid. People with this disease tend to be light sensitive. Treatment of this disease is difficult; contact lenses with an artificial iris help the condition by reducing the degree of glare.[33]

Nevi are benign pigment spots. They often occur in the iris and they are even used as features for identification. During puberty, these nevi can then increase in size and, in rare cases, develop into melanoma. It infiltrates the iris surroundings and can be malignant. However, due to the small danger of metastasis, there is no pressure to excise it.[33]

Chapter 3

Imaging the iris

The purpose of iris imaging can be divided into two large fields. One of them is **ophthalmology** (*ocular medicine*) and the second is **biometrics**. In the case of Ophthalmology, such emphasis is not placed on the detail of the picture, since most symptoms of Iris disease or injury are commonly visible. Biometrics, on the other hand, works the other way round. Details here are of the greatest importance as well as the speed of creating the image and its possible processing. Therefore, in bio-criteria, new ways are always being sought to image the human iris better. Out of the range of modern technologies and, most importantly, the reduction in the size of sensors, iris imaging can now be used as a security element in smartphones. Here, however, the speed of the system is placed above the reliability of imaging itself and the evaluation of the image. Therefore, they are built in such a way that the quality of the images is not especially good, but their evaluation is very fast. Most such systems usually do not even check features of the iris but rather the position of the pupil and other major parts of the eye.

Imaging can be divided into two main fields, according to the spectrum in which the iris is imaged. Imaging in light from the **near-infrared spectrum region**(*NIR*), this uses an infrared LED diode to illuminate the iris. This contributes to highlighting the distinctive features of the iris and ensures the overall purity of the image since there are not many disturbing elements in the imaged spectrum. However, the images that were taken in this spectrum lack colour information. This is the method is used most often as a bio-criteria. The counterbalancing this is imaging in **the visible light spectrum**(*ordinary light*). A classic camera or smartphone is enough to take such pictures. The biggest drawback of this solution is the volatility of the image quality, more specifically, the level of detail being such as to make it possible to evaluate the image. The quality of the picture depends on many factors. However, with proper picture quality and the level of detail, it can provide us with better information than the images taken in the infrared spectrum, in particular, information about colour.

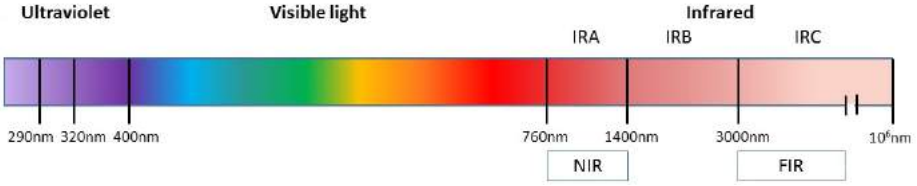

Figure 3.1: The light spectrum (taken from [1])

3.1 Infrared spectrum

NIR uses the 750 - 1400nm wavelength range, though, for imaging, a value of 850nm is used.[6] Radiation of this wavelength is not absorbed by melanin and, because of it, there is very good permeability even with a highly pigmented Iris (black eyes). Another indisputable advantage of this solution is that this wavelength does not dazzle the imaged person since the human the iris is not sensitive to this wavelength. However, this wavelength fails to provide sufficient information about the pigmentation itself. Most CCD sensors, however, are not adapted to image such a wavelength. Thus, while maintaining the desired quality, special equipment has to be used.[6] Other disadvantages associated with imaging are the necessity to take off the glasses or remove contact lenses; moreover, the human eye is not used to this wavelength. Instinctively, it is not so capable of reacting, for instance, by blinking. The maximum NIR illumination is set at 10 mW/cm^2.[3]

The imaging distance is limited to tens of centimetres. There is a considerable degree of unreliability in systems that use NIR during changes, for numerous inflammations or in removing the iris in people with translucent disability of the ophthalmic background or after cataract surgery. Systems using this method of imaging can be easily hacked thanks to very high-quality photographs or a contact lens with the iris printed on it. To reduce the likelihood of penetration, it helps detection.

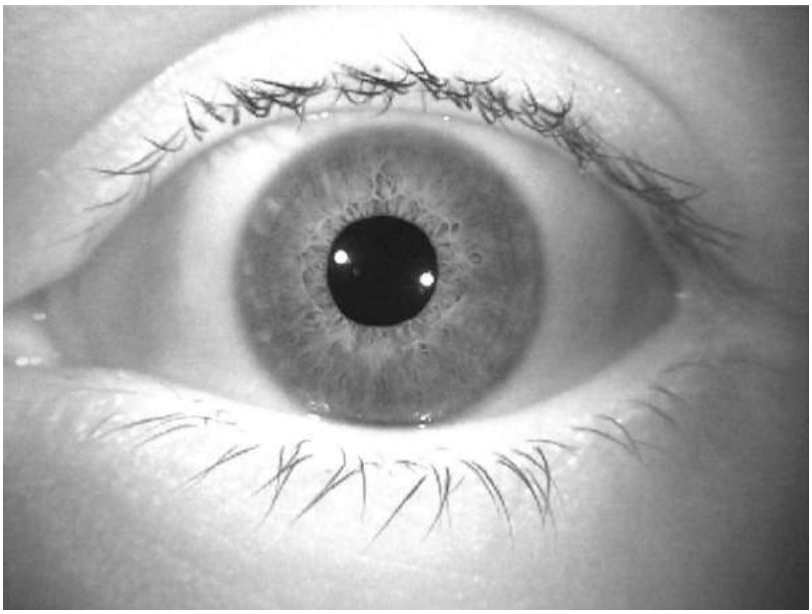

Figure 3.2: Sample image of the iris in NIR (taken from[23])

3.2 The visible spectrum

The 380 to 780nm wavelength spectrum is visible to the human eye. These wavelengths are successfully absorbed by the melanin in the iris of the eye and therefore, it does not obtain similar data quality as would be in the case of the NIR spectrum. However, this compensates for the fact that it is possible at this wavelength to transfer a large amount of information about pigmentation. The wavelength contains all the colour components that are needed to describe the colour of the iris. So then, it is possible in this spectrum to observe all the significant features that it contains. The level of detail is closely related to the sufficient intensity of the surrounding environment, in particular, to illuminate very pigmented irises, high intensity of additional light is needed.[3] In case of insufficient illumination, the noise of the image and its degradation come. It brings even more complications, because the human eye is sensitive to that wavelength and, from a certain intensity of light, imaging the subject's eye becomes uncomfortable and can be dangerous for the eye. Very often, quite a lot of light flaws appear in the images. These are caused by the reflection of some parts of the wavelength of the cornea. No special devices are needed to image the iris at this wavelength; it is enough to use ordinary CCD sensors.

NIR imaging suffers. For instance, printing a fake iris on paper or on the lens, which should then overlay the original one. The colour on both fakes will not be the same as in the case of the reference image (not even considering compensation). Thus, the need to test vivacity, due to suspicion, disappears in the fakes.

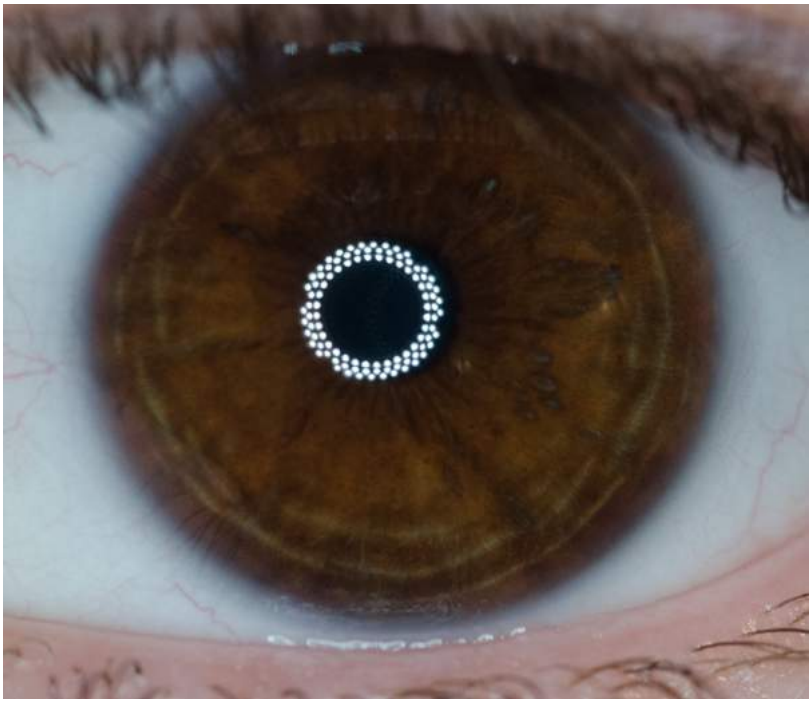

Figure 3.3: Demonstration of the iris image in the visible light spectrum

Chapter 4

Lighting

The design of the methodology for imaging in the visible light spectrum is a very demanding discipline. The visible spectrum has a lot of technical and, mainly, physical barriers, which should be taken into account right in the first draft of the entire methodology. One of the most important aspects is the sufficient intensity of light (*illumination*) of the iris. Thanks to the sufficient intensity of illumination acting on the iris, it is possible to extract more information from the details, which stand out in the visible spectrum and in this way achieve higher quality images than would be the case with the **NIR** spectrum.

Higher light intensity also largely contributes to the elimination of noise in the resulting images, a factor that mainly smaller sensor formats suffer from, with the so-called crop factor, than is in classic photographic film. However, the light intensity cannot be set too high, as it would lead to dazzle the imaged person, which means that there is a lot of brightness in the field of vision, or also there may be damage to organs of the eye. It is, therefore, necessary to find a compromise between a sufficient measure of light intensity and the comfortable median for the human eye.

The colour of the light colour or **chromatic temperature** must also be taken into consideration as this significantly affects the resulting colour of the image by transmitting colour contamination into it. This contamination then significantly degrades the informational value of the colour of the iris.

4.1 Light colour

Chromatic temperature is divided into 3 categories depending on how the given colour appears on the temperature range. These are **warm**, **neutral**, and **cold** colours. Warm colours typically have a temperature defined from 1000K to 4000K. Although this temperature range, which represents, for example, the heat of a candle or light bulb, is the most tolerated by the human eye, it adds too much colour contamination in the resulting images in the form of an orange-yellow tinge. The neutral temperature is represented by temperature in the range of 4000K-6500K. This range most faithfully simulates daytime white light that generates the slightest or no colour pollution (with the exception of extreme values). Cold light is defined by temperatures higher than 6500K. Such colour temperature of sunlight can typically be observed on a cloudy day or in foggy weather. Colour contamination is then generated in the form of a blue tinge.[31]

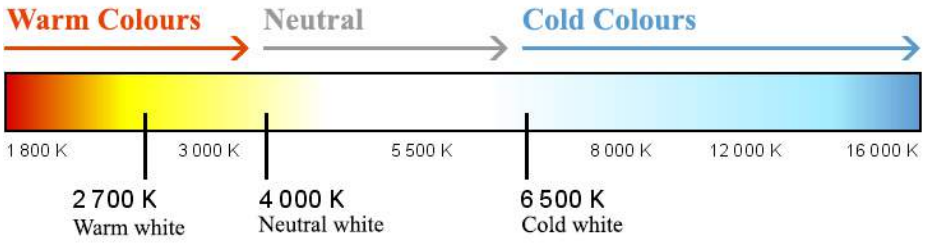

Figure 4.1: Range of colour temperature (taken from [31])

4.2 The degree of illumination

Imaging, as in the NIR spectrum, takes place at in close distance to the human eye. These are units of up to tens of centimetres. At such a small distance, it is necessary to take into account the thermal damage to the retina because of huge amounts of light falling on the lens, which is transformed into a single beam that is then focused on the retina of the eye. **Radiation intensity**(*Irradiance*) E_e (formula 4.1) is defined as the radiant flow on a unit area [W/m^2].[25]

The maximum intensity of such radiation is then defined by the European Union into two basic groups. *Group I* is limited by the maximum value of **1 mW/cm^2**, at this value, the human eye is not put to almost any physical stress and there is no threat of damage. *Group II* is defined by the following scale of values **1 - 10mW/cm^2**. The human eye here is then subjected to physical stress. However, more pronounced damage does not occur if the eye is not exposed to this for a long time. Values exceeding the limits of **10mW/cm^2** are very dangerous for the eye and permanent damage to the human eye occurs even during short-term exposure. These restrictions generally apply to the entire range of visible light and the NIR spectrum.[30]

$$E_e = \frac{\partial \Phi_e}{\partial A} \tag{4.1}$$

An important factor is also the total time of light flow from the light source to the eye of the imaged person. At this level, two different approaches are generally recognised. The first is short-term exposure (in the order of milliseconds) to extremely high light intensity. This approach is mainly used for photographic flashes when a very strong light is discharged for a short period. The duration of the discharge is then directly dependent on the exposure time. An extreme discharged light, though in a very brief flash of time, is very stressful for the eyes and unpleasant for the imaged person. The second approach exposes the imaged eye to long-term light radiation. The effective light intensity is then typically several times lower than in the first approach, and the eye is not subjected to such physical stress. The eye also adapts partially or completely after a certain time when the light source acts on it. Another advantage of this approach is the pupils are constantly contracted (more in chapter 2.2) therefore a larger area of the iris can be seen, which provides more information. In the first approach, the rapid transition from insufficient light to a large amount of light as result of the discharge may cause the pupil not having enough time to contract to their original status and thus depriving us of information. Its behaviour can be observed in the left image from figure 4.2, which was taken using a flash system. Thus, it can be seen that the pupil did not contract quickly enough to its normal size. In this image, the lack of light intensity can also be seen; this causes a low level of detail, and hence poor image quality. On the contrary, in the image on the right in figure 4.2, it can be seen that the pupil has a standard size and the illumination intensity is enough to be able to see all needed levels of detail.

Figure 4.2: Comparison of photos with differing intensities of light source.

4.3 Proposal

First, it is necessary to express mathematically and, after that, to determine the necessary intensity of light. The intensity of light must then be converted to the intensity of radiation and verified that it does not exceed the permitted limits and therefore that the health of the imaged person cannot be compromised. For the mathematical expression will be used features and formulas for calculating the exposure time, where they are used the basic exposure value, therefore, if required the intensity was higher than the permit limits, it will be necessary to adjust the basic value of the exposure time and slightly reduce the quality of the images.

Exposure is the amount of light per area. More precisely, the amount of light that for a certain time will act on the image sensor. This value is significantly influenced by the shutter speed, which indicates how long it is opened, and therefore the light can flow to the sensor. The second value that affects exposure is the lens aperture, which behaves similarly to the pupil in the human eye and allows in only as much light as its value indicates. It regulates the amount of light with the help slat that reduces or enlarge the aperture which can light rays can flow through. The value of the aperture also, to some extent, affects the depth of sharpness of the image. Its value then, in the end, is constant. To some extent, the shutter speed is also constant, which must be very small, thanks to the micro-movements of the eye. Over time, this would lead to detail blurring. The exposure value **EV** is acquired by applying the formula 4.2, **N** designates the aperture value and **t** is the shutter speed. Thanks to the exposure value, it is easy to calculate the necessary light intensity **E** using formula 4.3. It can also be expressed using brightness **L** and the following formula 4.4.

$$EV = log_2 \frac{N^2}{t} \tag{4.2}$$

$$E = 2.5 \times 2^{EV} \tag{4.3}$$

$$L = 2^{EV-3} \tag{4.4}$$

Due to constant illumination, unwanted reflections in the eye will occur. Since these reflections cannot be significantly prevented, at least they should be directed away from the iris, preferably into the pupillary part of the eye. This will keep images made clean and without loss of information. For this reason, a circular-shaped light source is chosen, which is placed directly on the lens, thus using the principle of a macro flash. This ensures that an imaged person staring directly into the centre of the lens has the light source projected directly into their pupil. It is also necessary that the outside diameter of the source is not too large and does not exceed the size of the pupil, which would then be contracted in that case.

When creating a depth map, it is necessary to create the largest set of images of one iris with different depths of field. Using an algorithm, the image sets are then combined into a single image with continuous depth of field. Such a connection is very demanding and it is necessary to detect edges or points that will then be used to compose individual frames. Artificial anchor points have to be made. These will take the form of colour diodes that are placed in the shape of a symmetrical cross. Always the same colour diodes are found on the vertices and horizontals. In the case of design 4.3, the red diode is on the vertical and green on the horizontal.

5500K LEDs provide the light source itself, this temperature is generally used as a source of neutral white light. As can be seen in design 4.3, the LED diodes are placed in double-rows with no diodes overlapping. This allows for the creation of continuous light around the entire circumference of the ring. The double row then allows for a change in intensity by activating and possibly deactivating individual rows. The source itself then must be diffused. However, a central diffuser cannot be used, as it would obscure the colour diodes. It is, therefore, necessary to select diodes that are already diffused.

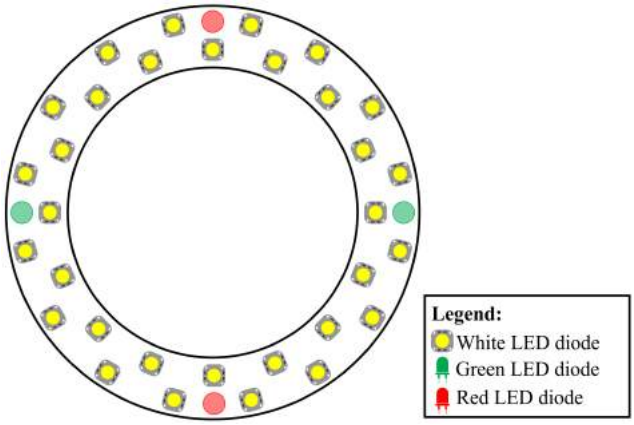

Figure 4.3: Desing circular lightning

Chapter 5

Methodology

Since there are not many specialised articles or information covering this issue, the theoretical basis for the methodology has to be derived from other sectors. Then, various combinations or variations of this information have to be made to meet the needs of this methodology. Information is drawn mainly from the fields of photography, physics and ophthalmology. As with any industry, there are exceptions that confirm the rule. Theories exist that are deliberately violated, especially when it is necessary to transform certain methods such that they can be combined with others.

Thus, the theoretical base only determines the outlines (boundaries) within which it is necessary to stick in order to achieve the desired results. The exact or, at least, similar data can then only be reached by empirical research. Therefore, established theories, as outlined in Chapters 3 and 4, cannot be fully relied upon, but rather taken as a basis for help. Often, while the methodology was being developed, changes were made to the original thesis and sometimes these proved to be impractical or did not lead to the desired results. Changes have often been iterative, as many of them came about only after thorough investigation.

As the imaging and development of some of the necessary components are still ongoing, the methodology can be considered experimental. Therefore, it cannot be stated that identical results will be reached if any other than the described or modified components will be used. Identical results may not be reached even when using precisely described components because there are too many factors that can affect the result. We will try to eliminate these factors by narrowly specifying the complete set-up of all components to avoid greater data diversity.

5.1 Lighting

The first important step in the methodology was to rework the lighting. This greatly affects the quality of imaged pictures. Whether it be 'readability' of the minutiae in the iris or colour contamination of the resulting image and the significant damage to one of the major minutiae - the colour of the iris. See Chapter 4 for more information on these consequences.

As a solution, the commercially readily available **Aputure Amaran Halo AHL-HN100 LED Light Macro** was used for the initial set of test images. Even though this light is intended for taking macro shots, it has proved to be unsuitable for our purposes. On the one hand, its maximum intensity of permanent illumination was not sufficient, but also the accessory flash, which was designed to simulate lightning, did not work. It was too aggressive and irritated the eye. In addition, its intensity was not sufficient, as the discharge time was much shorter than that of standard flashes. Removing the plastic diffuser did not help either. The intensity of illumination has increased, but it has still did not reach the required threshold that was needed. However, this commercial solution has served to design a custom solution. Its initial design can be found in the theoretical section in Chapter 4.3.

5.1.1 Changes from design

The resulting lighting has undergone considerable changes, mainly because the original design planned with separate LED diodes. However, in practice, these are not very useful nor are they commercially readily available. The following changes to the original design were the most significant:

- **Removing coloured LED diodes -** The circular base is equipped with LED tapes, so when adding separate marker LEDs the tapes have to be interrupted, connected to a separate colour LED and then reconnected to the tape. In addition, when changing intensity (voltage) of the LED tapes, the intensity of the auxiliary LEDs would also decrease, their meaning would then lose value.
- **Removing the LED diode chessboard layout -** In the original design, the LED diodes were arranged in a chessboard layout. This arrangement using LED tapes is not possible and the tapes were then mounted in three concentric circles around an inner circle. This allows uniform intensity throughout the entire length.
- **Use of a permanent power source -** Although the battery version would allow the entire setup to be more flexible, making such a device would be costly and impractical. When using a constant power source, various techniques can be used to modulate the intensity. For example a**DIMMER**, which allows for regulation of intensity. A similar mechanism can be used for battery systems, but these are technically and financially more demanding and do not reach such qualities as a constant power source.

5.1.2 Prototype

As has already been mentioned, the prototype is based on a commercial solution from which is draws mainly its shape and general functionality. The shape is annular because such a shape can be easily placed in the pupil. There will be no loss of data in the iris due to the light source overlap. The internal power then allows the light to be placed directly on the lens. This creates direct illumination of the iris. There is no need to position the eye or user. By looking directly into the lens, we maximize the amount of data in the iris and eliminate the unwanted glare that arises due to corneal rounding when viewed indirectly.

2mm-thick plexiglass was used for the prototype ring base. The diameter of its inner ring is 8cm so that it can be placed on the used lens. The total ring diameter is 18cm. There are LED tapes with **SMD LED diodes of type 5730** on it. These are placed in three concentric circles, as shown in the figure below.5.1

Figure 5.1: LED tapes on a plastic annular base

These, according to specification, have the input power set at **14,4W** per meter tape, being used with **1,5m** of LED tape being used, with an overall output is around **22W**. The temperature is then declared between the values **6000 - 6500K**, which was not the originally stated value for the design. However, this slight colour shift is calculated in the post-production part and will be compensated. The angle of light of each LED diode is then **120°**. This ensures greater light scattering and thus less light intensity, which reduces the eye stress factor. The luminous flux is then given with a value of **1200lm** per meter of LED tape. The total radiation intensity, at maximum power incident on the eye, is not higher than **2,2mW/m^2**, which is equal to risk group II (see chapter 4.2).

Since the prototype will only be used in laboratory conditions, it was possible to use LED tapes that have only **IP20** protection. The **IP20** degree of protection refers to an *electrical device that adequately protects against electric shock from dangerous contact with the finger*. It is resistant to the penetration by small foreign objects and is not protected against water.[14] The power supply is then provided by means of **12V** DC voltage, which is controlled by the so-called *„DIMMER“* (shown in Figure 5.2). It can regulate the supply voltage in the range of **3 - 12V**, which allows for the manipulation of light intensity. Another thing that was not needed in the laboratory and, mainly, in testing conditions was LED diode cooling, itself. These tend to overheat over longer periods (more than 20 minutes), which does not help their performance and, in particular, lifespan.

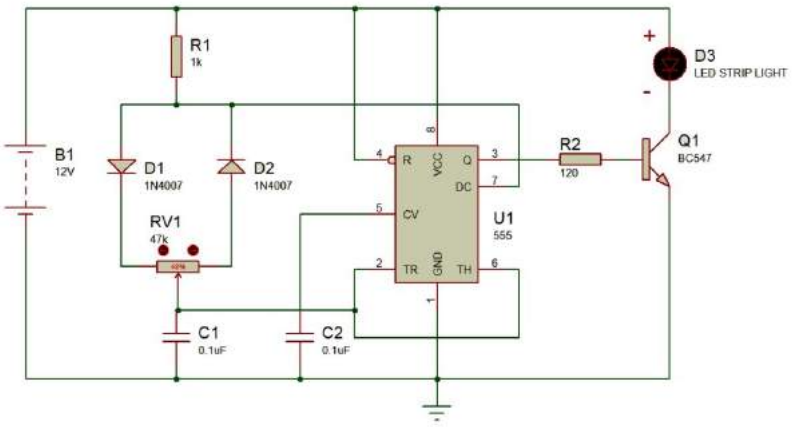

Figure 5.2: Prototype wiring diagram

The prototype is equipped with a temporary diffuser. One of the reasons being because of the softening of the light, which should significantly reduce the physical stress to which the eye is exposed and, secondly, because of the greater light scattering. For the time being, a diffuser made of white, waxed baking paper was used as it has similar optical properties to translucent, diffusing plexiglass, which would be time-consuming and financially demanding for the purposes of this prototype. This technique is widely used in photography.[28]

5.1.3 Prototype testing

After putting together the first lighting prototype, it had to be thoroughly tested. Given the time constraints that arose because the prototype took too long to make, it was clear that it would not be possible to produce original lighting from the prototype. The prototype was then used for all other imaging, or it underwent minor modifications. The first extensive testing found several bugs that had to be resolved on the go:

- **Flickering LED diode -** This is a well-known phenomenon, as seen in Figure 5.3. It occurs when using LED lights that are connected to the mains. This is caused by cyclic voltage. The current is reduced to a value that does not keep the LED lit up, so the LED turns off, creating a flicker. Typically, the network is under a voltage of **230V** at a frequency of **50Hz**. Such a voltage has a characteristic sine wave, so within the space of a second, its value is zero twice. This may cause some interference in the circuit behind the power supply. The dimmer interrupts the power supply to the LED tapes, thereby controlling the current flow, causing a fluctuating change in light intensity. This multiplies the frequency of this phenomenon. One way to reduce this phenomenon is to remove the dimmer from the setup prototype. However, this results in not being able to adjust light intensity. Other options include using ballast, the installation of which would be too demanding in the prototype. The use of a capacitor that would be placed on a dimmer would greatly reduce voltage fluctuations. The most effective option is to change the camera settings to eliminate this effect. More in the chapter 5.2.3.

- **Unsatisfactory size -** Originally, the prototype was designed for a different lens and camera. This setup had a greater minimum focal length. This was also in relation to the greater distance of the light source from the imaged eye. This problem can be solved by moving the light on the lens closer to the camera (i.e. away from the eye) and increasing the light intensity.

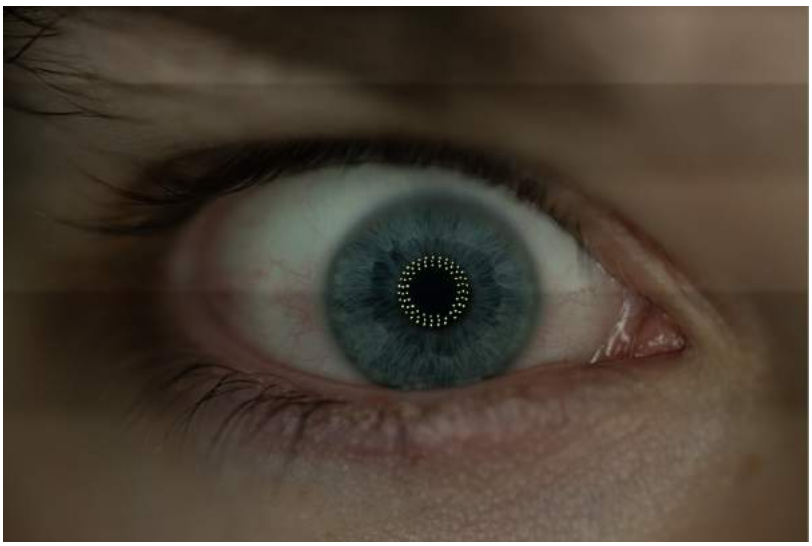

Figure 5.3: An example of a flickering fragment in a photography

When creating a test set of images, the prototype intensity was set to **1/3 of its maximum power** after the first series of tests even with the diffuser attached. This output produced almost no physical stress to the eye, so it was possible to keep the eye open at all times. For better results, it is advisable to increase the light output setting. However, greater light intensity caused a tendency for the subject to close the imaged eye to regulate the greater intensity of light flowing on the retina. Thus, there was no direct exposure of the eye to excessive stress, but evoked a condition that only caused a defensive response. The layered diffuser could then lead to softer light and hence the ability to set the output to higher required values.

5.1.4 Prototype modification

The most important modification of the prototype will be the replacement of the plexiglass mat and the installation of LED tapes into the printed circuit. This will solve the diode-cooling problem. In addition, the individual mounted diodes themselves will be improved. On the other side of the printed circuit board, an enhanced phase-dimming mechanism will be placed, which should eliminate the flickering problem. Thus, the amount of wiring will be reduced and the handling of the entire lighting system will be improved. The printed circuit board can then be inserted into a protective cage.

5.2 Technology

There was also a significant change in the technique used, as opposed to the proposed design. For example, a **Nikon D7000** camera with **Nikkor** and **Sigma** lenses was used to create the first set of tests. These lenses had different focal distances, more specifically *60mm*, *85mm*, *105mm*, and *150mm*. Both lenses have a *Micro/Macro* ratio of **1:1**. This ratio indicates that a 1mm physical object is projected exactly as 1mm on the camera chip, as can be seen in the example 5.4. Therefore, there is no reduction, so the image is not distorted and the necessary data is not lost. There is also the possibility of using Macro lenses with an **X:1** ratio, which allows further magnification and detail enhancement.[17] However, such lenses are expensive. Fortunately, they can be substituted- more in the chapter 5.2.3.

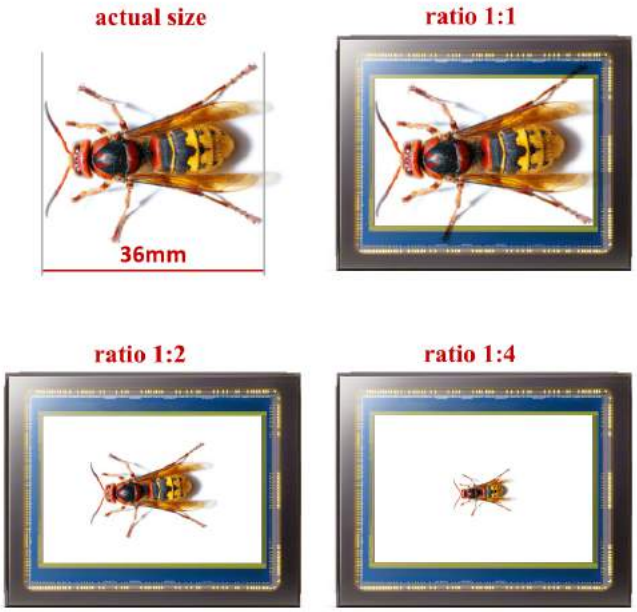

Figure 5.4: Chip magnification ratios taken from [15]

Then, it was found that the camera corpus, with its parameters, was insufficient. The chip is an **APS-C** chip. In the case of the Nikon, this means that the chip size is **1.5x** smaller than classic **35mm** film of dimension **24x36mm**. Such a chip reduction ratio is called the **crop factor**.[16] The advantage of chips with a crop factor is in the mentioned reduction, compared to film, in our case by 1.5. This factor increases the focal distance of the objects. This results in a narrower viewing angle of the camera while maintaining the declared minimum focusing distance. This phenomenon could then be described as a digital zoom, without loss of data quality and without noise in the resulting image. The chip in the camera used by the camera then has a resolution of only **16.2Mpx (i.e. 4928x3246)**. This significantly reduces the amount of data in the resulting image. Generally, APS-C chips suffer greatly from noise in dark parts of the image at higher **ISO values**, which also significantly reduces image quality. This fact is especially noticeable when a **1:1** image is enlarged (i.e. the full depiction in its real resolution).

The main specification for the choice of lens, apart from the focal distance that indicates the lens shot, was also the minimum focusing distance. This indicates at what minimum distance to the object that the lens can focus. This, together with the first specification, creates what amount of data is displayed on the resulting image. For example, using a lens with a focal distance of 150mm and a minimum focusing distance of 10cm may cause a problem. The lens would be so close to the iris that, at that distance of 10 cm and a focal distance of 150mm, part of the iris would be beyond the boundary of the sensor and would not be imaged. A state has to be reached, where the entire iris and the sclera are displayed on the sensor. This condition must be achieved at a distance that is indicated by the minimum focusing distance and at the appropriate focal distance of the lens. It would be ideal that other unnecessary parts of the face would not be seen, such as the arch of the eye or the root of the nose. This would be the perfect situation so as to obtain the maximum amount of information from the image. Therefore, in the initial phase, a number of lenses with varying focal distances were tested. The best images were provided by the **Sigma 150mm F/2.8 Macro** lens, with a focal distance of **225mm** after compensation for crop factor, and a minimum focusing distance of **38cm**. However, as can be seen in the picture5.5, there is still quite a bit of free space and the amount of acquired data is rather average.

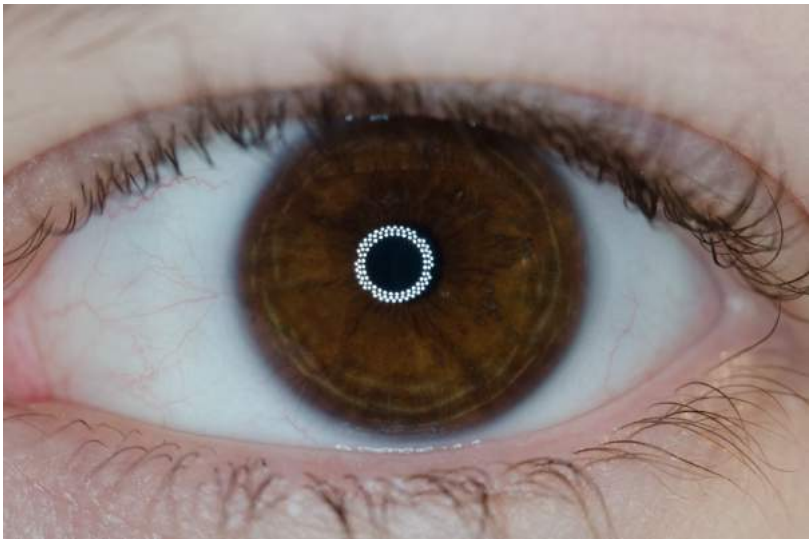

Figure 5.5: Image taken with a Sigma 150mm lens

5.2.1 Camera

As was mentioned earlier, it was necessary to find a more suitable corpus for the camera. Nowadays, there is a wealth of camera models from which to choose. Each of these models has its advantages and disadvantages and therefore it is not possible to identify the most suitable model. However, as a starting point, the requirements set by the specifications for the model should be taken into account. The first specification to be satisfied was that the new camera to be **FullFrame**, or textbf *„FF“*. Full Frame has a chip size equal to the size of 35mm film. With this specification, many models were eliminated as well as ensuring a higher quality of images, because Full Frame chips do not tend to create excessive noise in images.

Another specification was the size of the resolution. There was an effort to choose the model with the highest resolution and thus the greatest amount of information. The resolutions of such models range from **12Mpx** to **100Mpx**. 100Mpx models are usually quite hard to come by and very expensive. The last specification was good, low-noise image quality at higher ISO values. Only very few models matched these parameters, one of them being the **SONY A7R II**. It is a Full Frame, a **42Mpx** camera with excellent, high ISO image quality. This high resolution would allow us to make cut-outs from the resulting image without worrying about the loss of a large amount of data.

5.2.2 Lens

As a new corpus had been chosen, new lenses were also required, both because it is a completely different system, and therefore the previously used lenses cannot simply be fitted into the new corpus, and also because there is already a different sized chip mounted in it. The lens used, whose real focal distance after crop factor conversion was 225mm, should have, on this type of chip, its original value of 150mm. The choice of lens has narrowed only to lenses compatible with Sony systems. As mentioned above, it is impractical and unnecessary to mount third-party lenses through reductions if suitable native solutions exist. Therefore, it was necessary to find all suitable lenses labelled *Macro*. One of the few lenses then met all the required specifications was the **Sony FE 90mm f/2.8 Macro**. As its name suggests, its focal distance is 90mm and the minimum focusing distance is **28cm**. In addition, it allows the focusing distance to be reduced, which contributes to the precision of focusing at a very short distance. The magnification ratio for this lens is then **1:1**.

5.2.3 Settings

As with the prototype for the light source, it was necessary to properly test the new corpus and lens and establish the basic camera settings so that the images would be consistent. This will be done by ensuring four key settings:

- **White Balance Settings -** With this setting, we can compensate for the colour shift that arises due to the different light temperature (more in chapter 4.1). We know that the temperature of the LEDs used in the prototype is given within the range of **6000 – 6500K**. So we set the white balance to *6300K*. This ensures colour stability and credibility of all images taken independent of time, without the need for additional post-production. In picture 5.6 below, identical photos can be seen with different settings of the white balance settings.

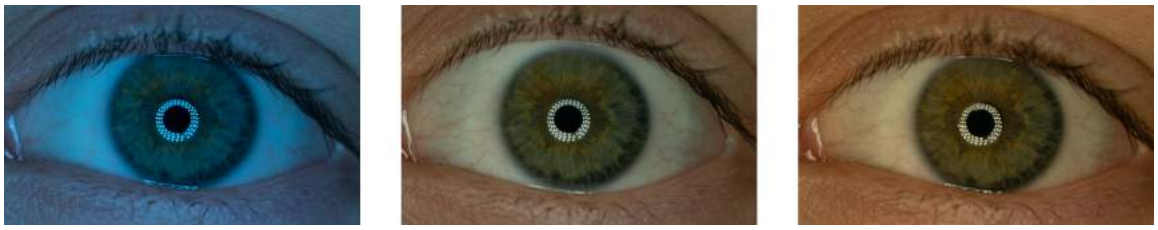

Figure 5.6: Different white balance values – *left*: 3000K, *middle*: 6300K, *right*: 9000K

- **Shutter speed (exposure time) -** It indicates the time that the shutter, located in front of the chip, is open so that the camera chip is exposed to light. This greatly affects the amount of incident light and thus how light or dark the photo is. Setting the shutter speed to **1/100** means then means that the shutter will only open for one-hundredth of a second. This exposure time will not allow in much light. On the other hand, a **15s** exposure time means that the shutter will open for a whole fifteen seconds, which is too long and allows a huge amount of light to reach the chip. When using the light prototype, we were forced to use an exposure time of **1/50**. This particular time, because the voltage that flows into the LEDs has a frequency of 50Hz, which is similar to that used for in high-speed flashes and so, flickering is not seen in the images. Alternatively, it is possible to use multiples of this synchronization value, where it is then possible to see minute traces of flickering, but it is not as significant as in other values.

- **Sensitivity -** Also called **ISO** in digital photography, is another aspect that determines the exposure (lightness) of the resulting image. In general, it is the ability of light-sensitive material to capture a certain level of light. The basic ISO value starts at 100 and the next value equal to twice the previous value, so 200. Each such value is then equal to half of the time needed to expose the image correctly. In addition, the lower the ISO value, the better the image. Since at higher ISO values, typically from **3200**, there is a large amount of noise in the images (visible in the picture 5.7), they significantly reduce the resulting quality. Because the exposure time is more or less fixed, the sensitivity will be significantly modified. Since the last specification also affects the overall exposure of the image, namely the aperture, ISO will have a relatively limited range of setup options. It will be necessary to set the ISO to a higher value. However, for the selected Sony corpus, this is not such a problem as the noise level at higher ISO values is not as significant as with other manufacturers. The values used are roughly in the range of 800 to 3200.

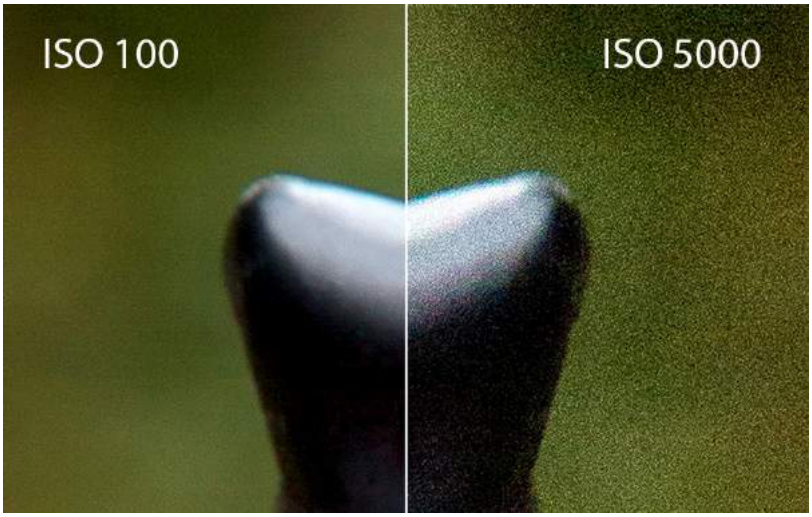

Figure 5.7: Visible noise at higher ISO parameter settings (taken from [20])

- **Aperture and aperture number (F) -** This works on a similar principle to the pupil in the human eye. It controls the amount of light that passes through the lens to the camera sensor. Just as a pupil regulates the amount of a stream of light by widening or contracting. The system of dilating and contracting stops, arranged in a circle within the lens, works in a similar manner. Furthermore, the number of stops in the system depends on how the lens was constructed. This number only affects the image cosmetically and in places outside the depth of field (in parts of the image without detail). So then, it is not necessary to pay particular attention to the number of stops. The aperture is the last aspect to influence the exposure of the image5.8. However, it does not only affect the exposure of the image, but also the overall depth of field5.9. This significantly affects the amount of detail in the image. As a general rule, the smaller the aperture number, the greater the depth of field and thus the smaller the amount of detail in images at different distances. The aperture size is given by the aperture number, F, which is written as follows: **F/2.8**. The digit after the slash then indicates the smallest possible aperture. In addition, the smaller the digit, the larger the aperture we can create, and more light that passes on the camera chip. The size of the aperture can then be expressed by the formula 5.1 where **F** is the aperture size, **f** is the focal length of the lens, and **d** is the diameter of the aperture opening.

$$F = \frac{f}{d} \tag{5.1}$$

A double aperture number means a quarter of the light let through. For this reason, apertures are designated as multiples of the square root of two. This corresponds to half the amount of light each time.

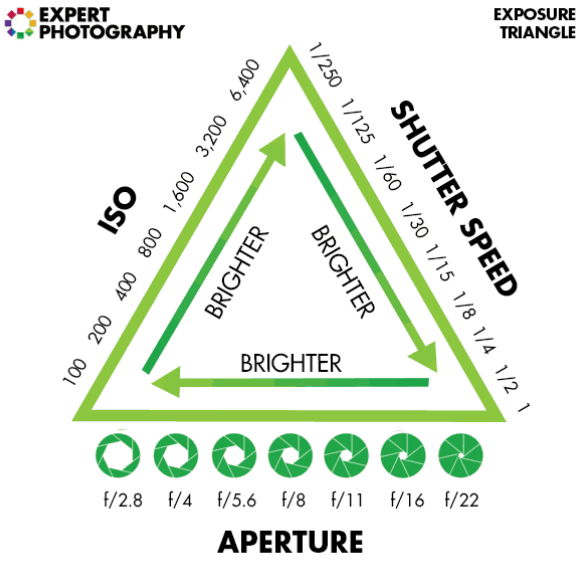

Figure 5.8: ISO parameter dependency, aperture and shutter speed (taken from [11])

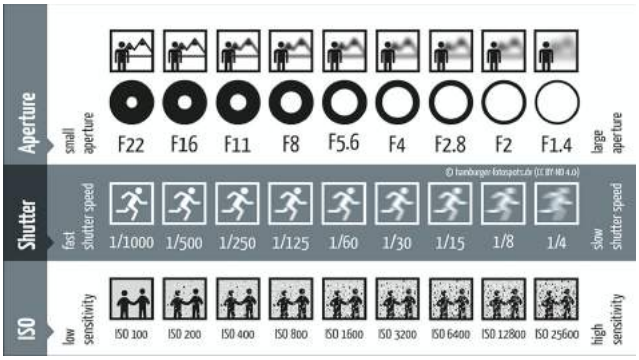

Figure 5.9: Image changes when setting individual parameters (taken from [10])

- **Depth of field** is the distance range (near distance for acceptable sharpness a far distance for acceptable sharpness) dividing the focal plane, which is determined by the focusing distance. However, the depth of field cannot be seen as a physical phenomenon, but rather as a subjective range of deviations from the focal plane. Thus, the expression of the principle on the human eye works, within the perception of detail, depending on the distance of the object. The extent of the depth of field is then influenced by 3 factors: **aperture**, **focal distance**, **distance**. Closing the aperture (increasing the aperture number) causes the light rays to be parallel, and thus the deviation from the focal plane is not so large, by which the depth of field increases. Conversely, when opening the aperture, the depth of field becomes smaller as the deviation from the focal plane increases. The shorter the focal length of the lens, or its focus, the greater the depth of field. Longer focal points then reduce the depth of field. For very long focal points or even telephoto lenses, the size of the depth of field range can only be **1 cm**. Finally, yet importantly, distance plays an important role. Here, the closer we are to the object, the smaller the depth of field and vice versa. Long-focus macro photography has its own specific features, where it reaches a very small aperture of **milli-to-micrometre** range depth of field. The size of the chip is such, that it does not have the depth of field. However, the crop factor can significantly increase the focus of the lens and significantly reduce the depth of field. A light spot passing through an unfocused lens appears on the sensor as a blurry circle. This circle is known as the **Circle of confusion (CoC)** and by its diameter, the size of the blur on the sensor can be measured. In an A4-sized image, the blur can be within the tolerance of 0.25 mm, which is the resolution of the human eye. Thus, if we reduce the size from A4 to a 35mm film size, which is 8.5x smaller, we obtain a CoC value for the FF sensor that comes to **0.0294mm** (0.25/8.5). Applying the same formula will also give the APS-C sensor value, which is **0.0195mm**.[22] In the case of the lens used at its highest possible depth of field, at an **F/2.8** aperture and a **28 cm** distance from the lens, this depth-of-field plane is only 1 millimetre. Gradual testing revealed that the ideal depth of field, at that distance of 28 cm, moves around the aperture number **F/6.3**. This is a depth of field of **2.5 millimetres**. The size was calculated using the formula 5.5 for which we needed formulas 5.2, 5.3 and 5.4. Where: **H** – hyper-focal distance [mm], **f** – focal lens distance [mm], **s** - focusing distance, $\mathbf{D}_n$ – the nearest sharp distance (is the nearest distance for acceptable sharpness), $\mathbf{D}_f$ – the furthest sharp distance (is the furthest distance for acceptable sharpness), **N** – aperture number (f – *number*), **c** – circle of confusion [mm] taken from [5]

$$F = \frac{f^2}{N * c} + f \tag{5.2}$$

$$D_n = \frac{s * (H - f)}{H + s - 2 * f} \tag{5.3}$$

$$D_f = \frac{s * (H - f)}{H - s} \tag{5.4}$$

$$DoF = D_f - D_n \tag{5.5}$$

- **FullFrame vs. APS-C mode:** As mentioned earlier, a camera with a 35mm film size chip, i.e. Full Frame, was chosen. This has indisputable advantages in better control over depth of field. Generally, it generates a higher resolution and has much less noise in images taken. Noise level and, subsequently, its reduction are both an essential factor since imaging takes place under laboratory conditions where no other light source is present, except for the developed prototype. Therefore, the images show a higher degree of noise. However, the selected camera corpus can also be switched to APS-C mode, which causes a crop factor of 1.5 to be activated and the resulting 42Mpx image resolution to be reduced to just 17.8Mpx. The software then records the data that would fit in the chip and discards the rest of the data. This mode allows us to extend the focal length of the lens from the original 90mm to 135mm along with a reduction in resolution. As a result, the coverage of the iris image is much greater than would be without using APS-C mode. However, there is more noise in the images. In picture 5.10 a difference can be seen in photos with APS-C switched on and without. In picture 5.11, a greater degree of detail can be observed in the case with APS-C mode switched off. When compared, the cutout from the photo taken from the Full Frame chip is enlarged 1:1 in proportion to the image taken with APS-C enabled mode.

Figure 5.10: Return mode images comparison. *Left:* APS-C mode, *Right:* Fullframe mode

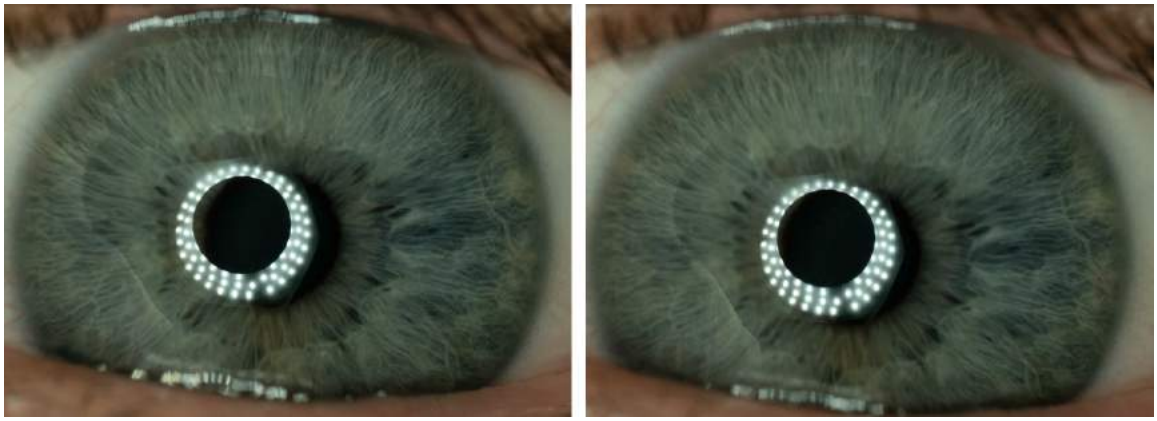

Figure 5.11: Comparing detail in a 1:1 ratio. *Left:* APS-C mode, *Right:* Fullframe mode

- **Focusing and magnification:** The original idea was to use autofocus. However, this proved to be a bad solution. Even the most advanced system was unable to focus on such a small distance as required. Another option was to use a systematic sequential lens-focusing ring. However, the necessary cameras API software from the manufacturer was not provided. The last method and the one that was used is manual focusing. Focusing is on at the minimum focusing distance and the iris is positioned exactly within this distance. The camera then allows the display to control the focal plane, which must be projected onto the iris. Due to the very shallow depth of field, only the iris and sclera are focused. Image quality is more than satisfactory, but at a **1:1** magnification, some of the markers in the eyes are so small that their differences disappear and therefore it is not possible to separate them properly. Nevertheless, they should interfere with far distance for acceptable sharpness. The laws of physics come into play here and the lens would need to be expanded to some extent. This reduces the minimum focusing distance and allows for better detail capture. Thus, it is possible to enrich the lens with a conversion lens, more precisely with a macro-lens or intermediate ring. The macro-lens works on the principle of a magnifying glass, which precedes the lens itself, allowing magnification greater than **1:1** mentioned in the chapter 5.2.3. The amount of magnification is then given in the **dioptres (+1, +2, +4, +10)**. Unfortunately, the macro lining has its ailments and the fact that in the final image a significant reduction of the drawing can be observed. As it is another optical element in the assembly, it brings with it a number of optical defects. The second option is the extension tubes. They look like a metal tube consisting of smaller sub-parts – an extension tube. The larger the extension rings (i.e. the lens distance from the chip), the closer the focusing distance of the lens is. Here it is possible to get to the minimum focusing distance in the order of cm. However, this also drastically reduces the depth of field and is very difficult to focus on very small points. Just like a macro-lens, it allows greater magnification than **1:1**, but at the expense of reducing the flow of light to the chip, which, in such difficult light conditions, creates another complication.

5.3 Summary

The methodology has undergone many iterations and its progress has changed many times, both significantly and slightly. The result, however, is a methodology for capturing high-quality images with great depth of field that encompasses all the details in the iris. The **Sony A7R II** camera with the **Sony FE 90mm f/2.8 Macro** lens was used to capture the images An experimental LED light circle of our own making was used as a source of light, the specification of which is described in chapter 5.1.2. The power intensity of the light source varies between *15 – 35%* of its maximum power. The scanned subject is seated in a special place with a padded back headrest to prevent unwanted head movements. The camera is then positioned at a height of the subject's eye, **28cm** from the iris of the scanned eye. In order to improve calibration accuracy of the minimum focusing distance of the lens, the focal area is displayed on the camera display. At this distance and the configuration settings described in the previous chapter, the resulting image is captured. When scanning the set for macro stacking, the stages with the lens out of focus have to be repeated until the focal area is projected onto the iris. Scanning takes place in a special room without any additional light source so as to achieve the most faithful colour reproduction and to prevent unwanted glare from another light source.

Chapter 6

Stacking and post-production

Using the technology and methods described in Chapter 5, we created a set of images where each image had a different depth of field. This means that, at particular points in the iris, the focal plane in a particular point of the iris occurs on the boundaries of focusing. Sharp and well-defined iris details are created between the far and near boundaries. In the parts of the iris that are beyond these focusing borders, detail defocusing (an effect called *„blurring“*) occurs, which leads to a significant loss in the value of information. The different image depths of field in the set should ensure that the focusing border always contains different details of the iris. These images make it possible to build a resulting image using one of the image-stacking or blending methods.

In such an image, the iris will be continuously focused, specifically, it will be properly focused over its entire area and contain the appropriate details at the desired level. Consequently, it is possible to work out the approximate distance from the first (base) photo from the plane of focus of the individual images and the steps of the lens-focusing mechanism. In this way, a concrete 3D model prototype with individual distances of detail levels in the iris can be created.

There are two possible approaches to handling the stacking itself. This can be either **manual** or **automatic** stacking. The first is completely in the hands of the user who only uses the appropriate graphical tools to implement stacking. It also uses subjective impressions and evaluating the quality of individual fragments of the images. Automatic, the second option is fully automated as its name suggests and inputs by the user are minimal. In this case, evaluating quality does not depend on subjective impressions but rather on strictly set criteria. The image sets have to be slightly correlated before applying either of these approaches. This means removing blurred, poor quality or damaged images, especially those that result from the movement of the eyeball or blinking of the eye. After correlation, in each set there should be at least three images, otherwise, no stacking methods can be used. Mainly, because of lack of information.

After applying either of the methods, we get significantly better and more readable details in the iris of the eye. In addition, these images contain information about distance and can be varied using different filters. Both of these methods have their undeniable advantages, but they also have specific disadvantages.

6.1 Manual stacking

This method requires a raster graphics editor that can handle individual layers in the image. Typical representatives of such editors are *Adobe Photoshop*, *GIMP* or *Affinity* and others. The first of the above mentioned was used as an editor in this work. Because of its ability to open the RAW format, it can save all the image source information and can be used in a non-destructive way and in addition, it has a wide range of filters that can greatly assist in stacking the individual images and evaluating fragments with details. A method with a precisely defined procedure to ensure that the resulting images remain unchanged has been designed:

- **Specifying the base image:** First, you need to specify the base or reference image. This serves as a basis for the correlation of images that will be performed later, at other points. The first image in the set is usually designated as the base image, assuming that it does not show any significant damage fragments (such as from blinking) or does not suffer from a lack of detail in the iris.
- **Focusing the iris:** Using the base image and, with the help of the ellipse tool, two elliptical shapes will be created in separate layers always at the top of the image 6.1. This ensures they are always visible. The first shape traces the outer edge of the iris and thus represents the boundary of the entire iris and hence its size. This size does not change and is crucial for later correlation of all images. The second shape is located on the inner edge of the iris, i.e. bordering the pupil. However, it has a variable dependency on time and on the intensity of light and might not always be the same size in the images. Because of this, it is used as an auxiliary indicator. If very detailed minutiae are visible in the iris, it can be marked with any shape that has directional markings, because of possible image rotation.

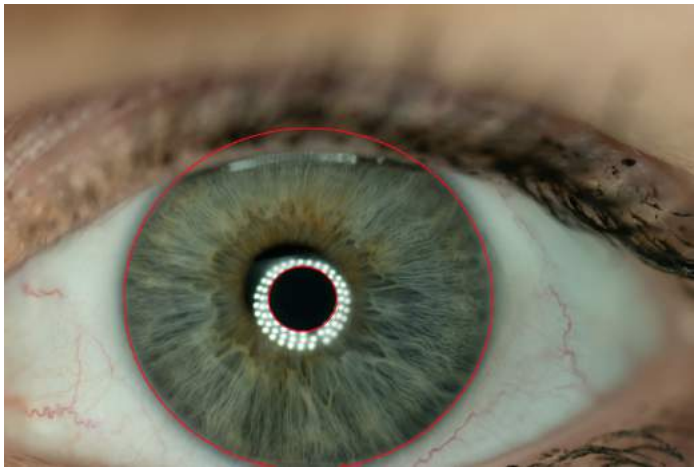

Figure 6.1: Identification of the iris on the base layer

- **Image correlation:** All the other images in the set are then inserted into the base image, individually, with a separate layer for each image. Iteratively, the individual layers are listed through and by shifting, or if need be, by adjusting the size or rotation of the images, the iris is placed to be within the marked elliptical shapes. This step creates an overlap of the individual irises.

- **Applying filters :** Separate filters are applied to each layer to refine the results and improve the visibility of each focused detail. The first filter is **High Pass**. In photography, it is mainly used for sharpening images. This filter only allows high frequencies through. This means, in practice, that only the sharpened fragments of the image will be displayed after applying such a filter. These show a high frequency in the image. The second filter is **Edge detection**. In images in general, the edge forms there, where there is a change in brightness, change in light, or the depth of the surface detail changes. Thanks to this filter, the sharpest details in the image appear. Both filters are applied independently of each other and each works with a different copy of the same layer. So, from one layer three are made. The base, on which no filter has been applied, the layer to which the **High Pass** filter has been applied and the layer with **Edge detection**. The latter two then undergo masking of unnecessary details6.2.

Figure 6.2: *Top*: Image after applying the High Pass filter. *Bottom*: Image after applying the Edge detection filter.

- **Creating a masking layer:** For each layer it is necessary to remove (delete) unnecessary details, i.e. blurred fragments of the image, and leave in the given layer just those that have the most informational value. Data in the layer should be kept for future use. Therefore, these fragments have to be made invisible instead of removing them. This is done by masking, which hides unnecessary portions of images in individual layers. The masking layer has a black background that marks the given parts that will not be visible. The visible parts are then marked white. Masked layers are created from copies of base layers that have had **High Pass** filters and **Edge detection** filters applied to them. The required details are labelled to create a detailed mask for each layer.

- **Finalising:** The masking layers created in previous point are gradually applied to all the layers except the base layer 6.3, which remains fully depicted; it is an underlying layer containing blurred fragments in the image. After the masking layers have been applied to the remaining layers, the desired details can be seen. Merging the individual layers creates the final image. In this case, two images are created. The first has masking layers created by applying the **High Pass** filter and the second has masking layers created by applying **Edge detection**. The third image is then created by combining both masking layers. The masking layer that was created by applying **Edge detection** is located above the layer that was created by applying the **High Pass** filter. This is because it contains a smaller set of details so it is important that the layer with a larger set of details does not overlap it. The result is, three images created using different methods.

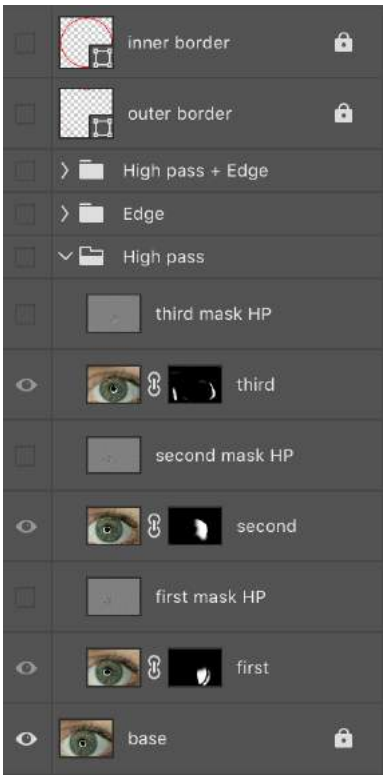

Figure 6.3: Individual layers before merging into a final image.

6.2 Automatic stacking

Unlike the first approach, it does not require user intervention or subjective assessment of the quality of individual images. In this, everything is done by the program. All the stages are automatic. Both methods are similar, the individual stages of the automatic method, however, are more complicated. In the first method, the graphical editor or the user has to carry out more tasks themselves. As an example, we can use the exact identification of the pupil and iris. Within manual stacking, the user is able to identify pupils and iris at first glance with 100% accuracy. However, automatic stacking requires a series of matrix image adjustments and subsequent pupil identification by circle detection. The pupil is used to get accurate identification of the iris, a process that can also be done using circle detection, which may not always be accurate, because in some photos the iris shows slight deformation and is therefore not an exact circular formation.

In particular, the image processing methods that are used are contained **in version 3.4.**, of the **openCV** library. In addition, the **numpy** library is used, mainly because of methods that allow work with matrices. The last, major library, **matplotlib**, used for displaying or comparing individual images that come from the given stages. **Version 3.7 of Python** is the chosen programming language. As has already been mentioned, the algorithm is almost identical to that in the first method. Enhanced functions that the user is used to have to be added to each individual stage but the program requires special, pre-prepared data. The algorithm can be divided as follows:

- **Image normalisation:** Since the images are not the same size, they need to be unified to an exact size. However, this must be set so that the images are not distorted the images maintain the correct aspect ratio. The aspect ratio is **3:2** and the standardized resolution is **1440x960px**. Pixels in all images are always divided by an even number so the pixels are halved, leading to unwanted image distortion and loss of detail.

- **Converting an image to grayscale and blurring:** Before identifying the pupil and the iris, the images still need to be adjusted. More precisely, the images have to be converted from the colour spectrum to grayscale. This is done using the **cvtColor()** function from the openCV library, expanded with the **COLOR_BGR2GRAY** function. It determines from what spectrum to which will the change be made. Converting an image to grayscale has numerous advantages. One of them is to highlight individual colour transitions. Also, make it stand out. Next, there is no need to identify the pupil and iris in all colour channels depending on the colour of the iris, but only one grayscale channel. Another important adjustment is blurring the image using the **GaussianBlur** function. Blurring reduces the number of tiny details and this significantly eliminates false-positive rates in determining pupils. The following equation 6.1 is used to express **GaussianBlur** in a 2D space. Sigma is then calculated using a **Kernel**, of size field **x*x**. According to which the given image is divided into blocks and the average value is calculated from them. A **kernel** of size **23*23px** is used to calculate our sigma. This provides us with optimal blurring.

$$G(x,y) = \frac{1}{2\pi\sigma^2} exp^{-\frac{x^2+y^2}{2\sigma^2}} \tag{6.1}$$

- **Pupil Identification:** One of the key methods. The position of the pupil has to be properly determined iris identification is derived from this. As the pupil is circular, it is possible to use **HoughCircles()** for identification. It works using circle detection, more precisely, identifying the circle centre and then the corresponding radius that surrounds the transition border between two edges. It is therefore important to set the following parameters:

  - *The minimal distance* between identified circles determines the distance that each circle must have between each other. Here it is set to **120px**
  - *Threshold edge (param1)* is the upper threshold for an internal edge detector. The boundary is set to a value of **55**
  - *Accumulator threshold (param2)* to detect the centre of the circle. The threshold for the centre is set to a value of **35**
  - *The minimal radius* of a detected circle
  - *The maximal radius* of a detected circle.

  Since pupil size is not known, both of these parameters are left to zero, thus unlimited. Thanks to these settings, the pupil can be identified very precisely. However, if the function returns multiple identified circles, the first identified one to be identified will be selected.

- **Applying a threshold:** Before the iris itself is identified; the image has to be adjusted using the threshold. This means that the pixel grey colour boundary has been selected and if the colour of the given pixel is larger, then in the case of the selected **THRESH_BINARY** parameter, the pixel is recolored to the set value and if its colour is set to **0**. This creates much sharper transitions and better iris identification.

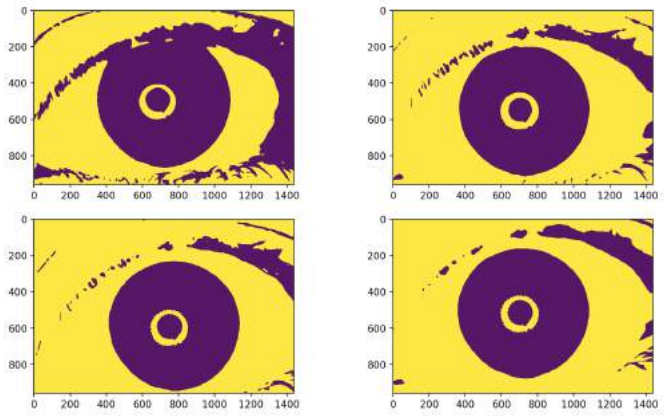

Figure 6.4: Images after applying a threshold

- **Aligning the images:** As has already been mentioned in the first method, all the images in the set have to be aligned to the first (baseline) image. The images are aligned (by shifting) to the coordinates of the centre of the base image using the **warpAffine()** method, which performs various geometric transformations depending on the value of the transformation matrix **2x3**.

$$\begin{vmatrix} 1 & 0 & s_x \\ 0 & 1 & s_y \end{vmatrix}$$

Where s_x and s_y are the differences of the base coordinates from the coordinates of the actual image. This value indicates how much the image has to be shifted within the given coordinate system. After applying this method, you also need to adjust the pupil and iris coordinates in the actual image.

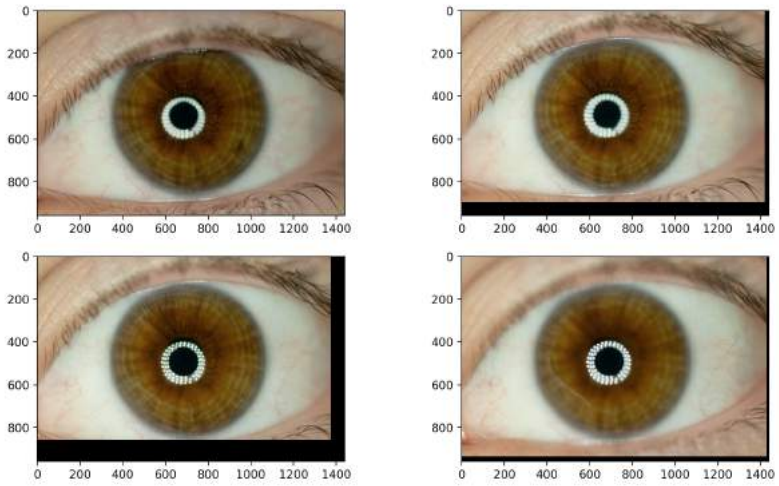

Figure 6.5: Sample of a base and a shifted images

- **Creating masks:** To identify and then align the irises in the set, you need to apply a mask to each image for better manipulation with the image. The result will then be an image that contains only the iris while the rest of the image is filled in with a black mask. This image editing will greatly help in creating a bitmap mask of focused image fragments. First, a matrix of zeros and frame size (i.e., black image) is created. This mask is drawn using acquired coordinates, circles, substitute irises and is then filled in with white colour. This creates a mask that only shows the iris. The **bitwise_and()** method executes a logical AND over the mask and frame. This creates a new image that only shows the iris.

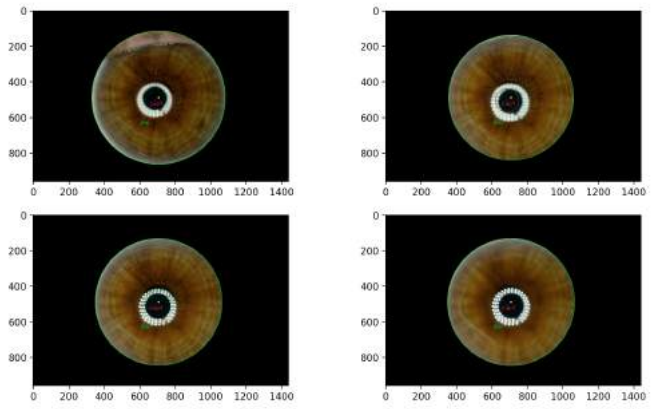

Figure 6.6: Iris clipping mask applied to an images

- **Bitmap:** Creating bitmap from focused fragments of individual irises. With each image in a given set, a bitmap is created, using the above-mentioned OpenCV library and edge detection functions or the **Canny()** function. Each image also contains information about the focal distance. This can be projected to the individual layers.

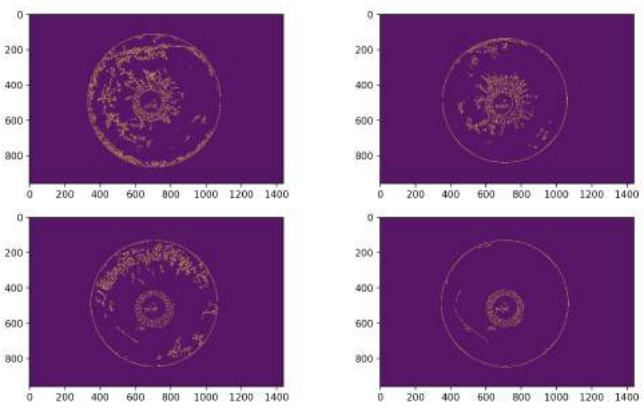

Figure 6.7: Images bitmap from a set

- **Finalizing the image:** The bitmaps of individual images (layers) are merged into the resulting image using a **logical AND**, creating a final image map containing all the focused fragments. The base image is the foundation, which complements the blurred fragments of the resulting image.

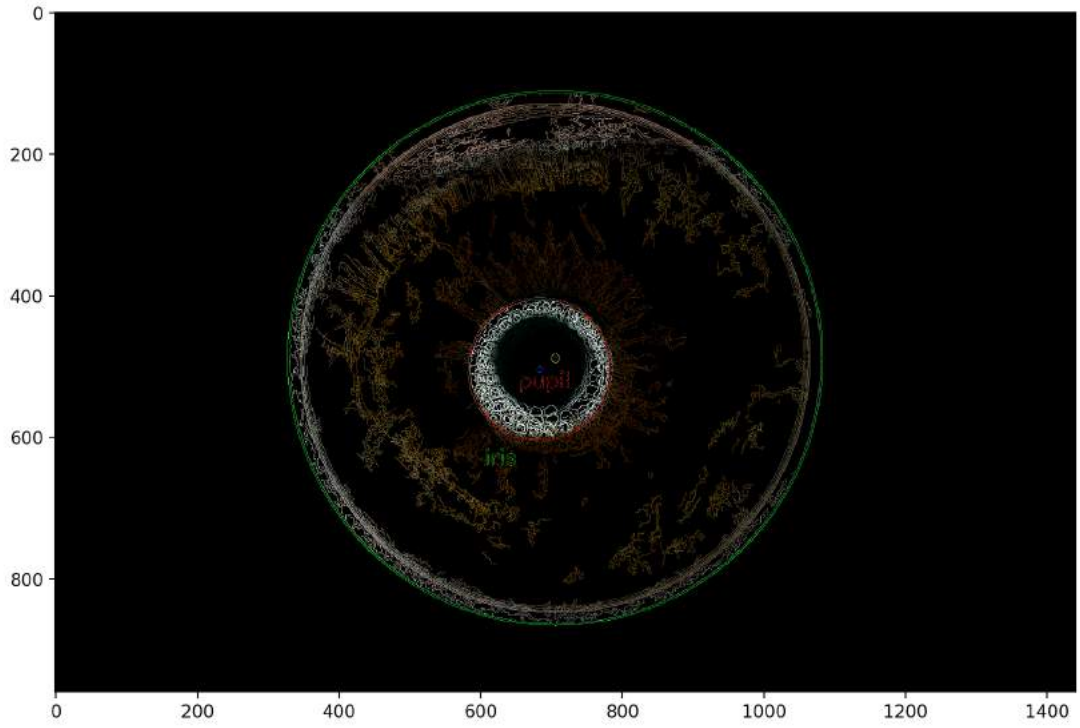

Figure 6.8: Final bitmap image

Testing

In automatic stacking, the script was applied to about 56 sets of frames that met the minimum requirements for using the stacking method. Of which about **69.7%** of the sets were correctly identified irises. In about **7.1%**, the algorithm was unable to cover the entire area of the iris, but determined its position correctly, with only an inadequate radius. Furthermore, about **23.2%** of the time, no iris was found at all, because of either not finding a suitable pupil or finding a corresponding circular shape that would fit the iris criteria.

6.3 Filters

As a result of the change in the method of taking the resulting images, it was necessary to add post-production filters that would eliminate the flaws of the newly selected method. These were mainly are filters for the elimination of colour noise, for example, a **Low-pass filter**, a **Gaussian filter** or one of the **Nonlinear filters** were used. Then there was the fine focusing of important parts of the image that contain the depth of field needed. This, for example, was a variation of the **High-pass filter**, which only allows through high frequencies that define in and image detail and proper space. This release of high frequency, however, is precisely the reason noise gets back into the image. Therefore, it was necessary to test and verify to what extent individual filters should be applied to the image in order to achieve the desired results. Experimenting with these filters led to the idea to apply other suitable filters, which could significantly contribute to highlighting the depth or pigment maps in the iris of the eye, and thus ensure a better readability of the minutiae in the iris, independently of the colour of the iris. The first experiment was conducted on the above-mentioned high-pass filter. This was not applied directly to the image, but a mask was created using the filter visible in picture 6.9.

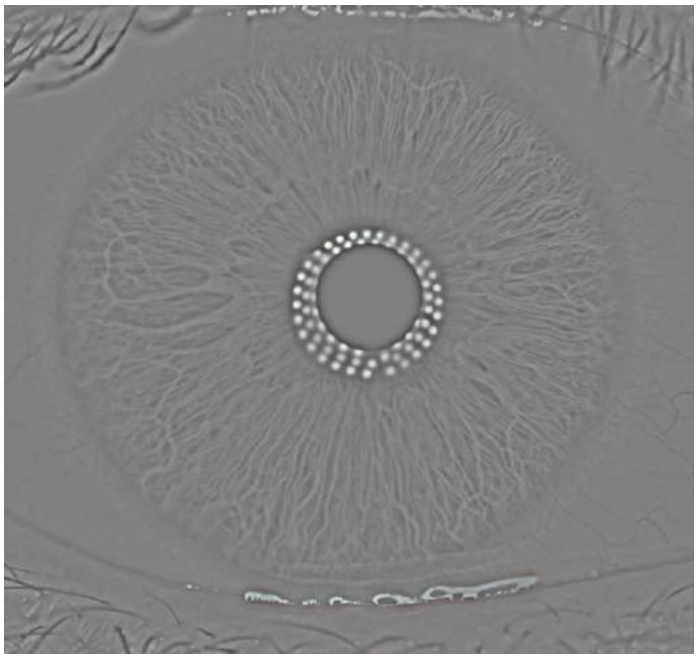

Figure 6.9: Creating an iris mask using a High-pass filter

Because of the change in the method of taking the resulting images, it was necessary to add post-production filters that would eliminate the flaws of the newly selected method. These were mainly are filters for the elimination of colour noise, for example, a **Low-pass filter**, a **Gaussian filter** or one of the **Nonlinear filters** were used. Then there was the fine focusing of important parts of the image that contain the depth of field needed. This, for example, was a variation of the **High-pass filter**, which only allows through high frequencies that define in and image detail and proper space. This release of high frequency, however, is precisely the reason noise gets back into the image. Therefore, it was necessary to test and verify to what extent individual filters should be applied to the image in order to achieve the desired results. Experimenting with these filters led to the idea to apply other suitable filters, which could significantly contribute to highlighting the depth of pigment maps in the iris of the eye, and thus ensure better readability of the minutiae in the iris, independently of the colour of the iris. The first experiment was conducted on the above-mentioned high-pass filter. This was not applied directly to the image, but a mask was created using the filter visible in the picture 6.9.

Because the images are taken in the visible spectrum, they contain information about the colour structure of the iris; it is possible to experiment with filters and methods that influence the colour channels in the image. Depending on the colour of the iris, colour channels can then be removed that do not affect the colour and thus achieve cleaner and more readable markers in the iris. For example, removing the green and red channels, in the case of blue eyes and, in the case of brown eyes, removing the blue and green channels as shown in the picture6.10.

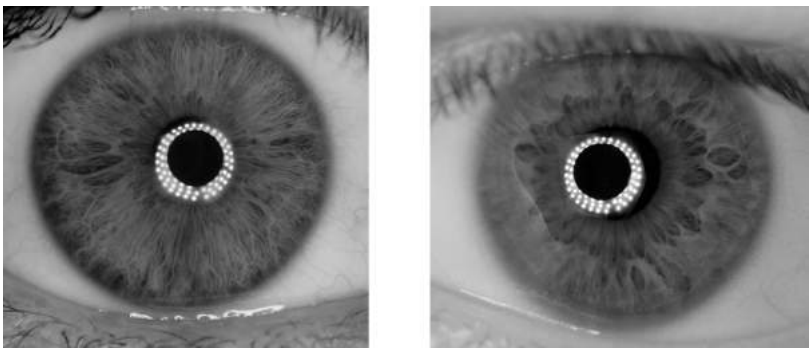

Figure 6.10: An example of the elimination of colour channels to highlight the structure of markers

Experiments can also be done with masking the main iris colour. This creates an inverted image on which the structure of the markers can be observed, which is normally hidden just below the colour part of the iris. However, masking cannot be applied to all iris colours or iris types. The best inverse map is achieved when applied to monochrome irises as shown in Figure 6.11.

Figure 6.11: Selective masking of the main colour of the iris. *Top*: Masking the blue colour in blue eyes. *Bottom*: Masking the yellow colour in brown-green eyes.

By variations and layering of individual filters and methods, countless new possible filters can be obtained, but most of the resulting filters do not meet the needs of the research and rather degrade the informative value of the image. Another possible modification of images is, for example creating colour maps.

Because of their high resolution, the images offer a great opportunity to experiment as they contain lots of source data. Even when applying extreme or invasive local filters, modifying portions of the image does not only result in degeneration or in data loss. Filters and image manipulation can be applied without loss of quality because the data is available in the **RAW format** that retains all the necessary source data, so there is no problem to recover part of the information if needed.

Chapter 7

Evaluation

Before comparing individual methods and approaches, criteria that are important to the project have to be defined. Since each method has its own specifics, they cannot be compared directly. The primary aim of the work was to create a methodology to capture and subsequently create a depth map. The first criterion then will be the **quality of the depth map**, specifically, the degree of detail that can be read from the images. Another important point was also the design of a lighting source to be used in taking the pictures. The aim, then, was to develop a source of lighting that would cause the least possible **physical stress** to the eye. The last important criterion is the difficulty of taking pictures in relation to the amount of information obtained. These three criteria should serve as the main indicator of the fulfilment of the potential of the described methodology in comparison with already existing or emerging methods. An additional factor may be the individual incomparable advantages and disadvantages of each method, such as the processing time or the time it takes for the imaging itself and other nuances. Since the iris is considered personal information, it is also protected, so most databases are not publicly available. Therefore, for comparison, we will only use available data.

7.1 Infrared systems

Generally, systems using this principle do not have a colour component in the resulting image, thanks to the use of a near-infrared beam. On the other hand, this should illuminate the iris better and the markers in the eye should be seen more clearly in the image. Moreover, the beam is not visible to the human eye, so there is no conscious exposure of the eye to physical stress. In addition, as can be seen in the images from the database created by the *Computer Vision Laboratory* at T*The Chinese University of Hong Kong* (available from [9]), the pupil is not always dilated to its maximum. This means that in some images, the structure of the iris is not fully seen and so there is a significant loss of information. Although there is no visible colour in the images, according to typical markers and iris shapes it can be assumed that the system has a problem with darker iris colours that contain almost no information, as seen in the sample picture7.1 from the database. In addition, the images reach a maximum resolution of **300x420px**. The *IIT Delhi Iris Database* (available from [13]) has a similar resolution. However, compared to the first database, the sample data shows a greater degree of detail, primarily in light irises. It can also be observed that the pupil is not sufficiently contracted for the images, so information is lost again for some of the images.

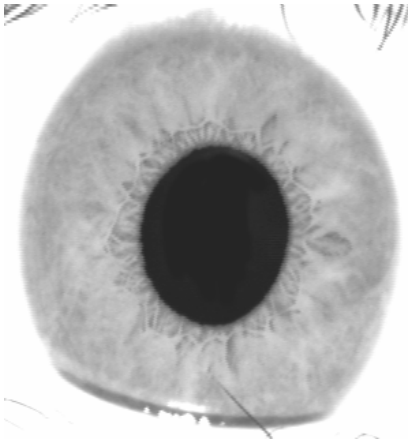

Figure 7.1: Sample image from *The Chinese University of Hong Kong* database available at [9]

Thus, it can be said that methods that use the NIR principle are the most appropriate for the perceived stress factor for the eye. However, in terms of quality, it is not sufficient. Images taken with this method are not constant, considering the different pupil size in each image. The image also lacks colour information, which for us is important. The image quality is consistent with system complexity. The imaging itself can then be performed anywhere indoors, using only special, portable camera technology.

7.2 Systems using visible spectrum

The main idea of imaging, in the visible spectrum, is to capture iris colour information that is completely missing from the NIR systems mentioned above. Due to the low-resolution rate, NIR imaging time is much better. Now, with the advent of more modern technologies and, above all, the increase in resolution, images in the visible spectrum, in terms of detail, have significantly improved. A continuing problem is a need for intense lighting in this type of imaging. This is both a technological problem and the imaged iris is exposed to a higher rate of more physical stress than when using NIR. Systems that use this principle can be divided into two basic types according to the imaging technology used:

7.2.1 Cameras

These systems use a standard **CCD** or **CMOS** chip to capture images, either embedded in a commercially available corpus or embedded in special hardware. The sensor is then connected to a special instrument that resembles a lens housing that consists of a system of lenses, mirrors and interior lighting. This device in ophthalmology is called a fundus camera7.2. However, it is used primarily to capture the retina.

Figure 7.2: Canon Fundus Camera (taken from [29])

However, the device can also be modified to capture the iris, which is can be seen by the Iris database, created at *Palacký University in Olomouc*, with the help of a similar device. In sample7.3, a very good level of detail can be seen irrespective of the iris colour. Moreover, the quality of the database is constant, but all the images suffer from a strange colour haze. Thus, when using iris colour as another marker, distortion may occur. The size of the images depends on the imaging sensor used. Here, it is **768x576px** which is very good value.

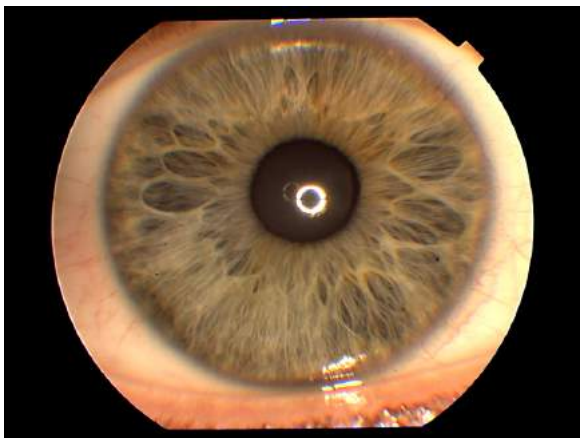

Figure 7.3: Sample image from database available at [4]

In general, systems using CCD or CMOS chips have the best results. In contrast to the system described in the work, however, a few details can be observed. The fundus camera system allows the imaged person more comfort in the form of a headrest and, generally, faster imaging. However, the colour contamination of the frames and the high level of eye stress factor play a detrimental role, as the lighting system uses a lighting discharge that is short but an extreme strain to the eye. Fundus cameras or a similar system is not very portable.

7.2.2 Digital Microscope

Systems operating on a similar principle to those using cameras. However, here the digital chip scans the image magnified by a special optical system. With this magnification, it achieves the best-detailed result of the iris. However, handling is demanding and the whole process of iris imaging is the most demanding of all presented methods. It is also necessary to illuminate the iris correctly and, because the microscope is placed in the immediate vicinity of the iris, there is a very high exposure to eye stress. Moreover, from such a distance, the reflection of the light is not only reflected in the pupil, but also in the iris, and data is lost, as can be seen in the top picture7.4. The eye can be imaged even without suitable lighting. In this case, however, other light sources are reflected in the iris, as shown in the bottom picture7.4. Although the microscope gives the most detailed iris image, thanks to the surprisingly high resolution of **1280x1024**, its manipulation and physical stress caused to the eye greatly reduces its ability to be used in a practical environment.

Figure 7.4: Example of images taken with a digital microscope in a biometric lab **STRaDe**

7.3 Results

Both methods showed satisfactory results but mainly generated information that could lead to their improvement in the future. An example is a shared hitch that comes from the high degree of image normalisation needed to be even able to perform these methods. Eye movement between refocusing and taking individual images of the eye is another drawback. Unfortunately, the solution cannot be used in the proposed methodology. It multiple sensors would be needed to capture differently focused images at the same time.

7.3.1 Manual method

In this photo-stacking method, 3 approaches were used: a **High pass** filter, **Edge detection** and combination of the two. These methods produced significantly varied results so suitable criteria for matching the results had to be chosen. The first criterion is a visual analysis of the images. It immediately suggests that all 3 approaches add false details to the image, mainly because of the eyeball shift and the delay between individual images. Therefore, a new criterion has to be chosen to show which of the approaches adds the most focused fragments to the base image. For this purpose, a script was created using the

Laplacian openCV library function. This parses the frame and returns a decimal floating-point value. The larger the output value, the more focused is the data in the image. As a result, individual stacking approaches can be mutually evaluated. This is also a reference image in the table 7.1 that has a huge depth of field with all the needed iris details.

As can be seen from the table, the reference image has a much higher value. This is because the image contains details outside the iris, which is not important for the measurement. A possible solution would be to apply a clipping mask to the iris and calculate the value again.This solution, however, is unnecessarily complicated, seeing as this is only a reference. Furthermore, the data shows that the most successful approach is to use the **High pass** filter, which was evaluated as giving the most focused image in **56%** of cases; the second was the **Edge detection** approach with **36%** and the least reliable approach was using a combination of the two in **8%** of cases, i.e. **only 4 images**. Part of the success of the **High pass** filter is due to the prevailing number of dark eyes on which this approach is very reliable. Next is an analysis of the unified properties of filters and their disadvantages:

- **Edge detection:** Applying this approach to light irises, namely light blue, blue, light green, teal, or grey-tinted irises gives better results. On dark-coloured irises, specifically, green, dark green, green-yellow, dark blue, or any brown coloured, the results are significantly worse. This is due to the contrast of the individual minutiae in the iris. In bright eyes, there is a greater contrast and the Edge detection filter transforms this contrast into sharp outlines better. The filter overlaps the image with white. Thanks to the contrast, the edges stand out. It works best on the iris, where contrast constantly changes, which is the case with light colours. In dark irises, the contrast is not so great and so, after applying the filters, not as many sharp edges stand out. Often, in such dark irises, the filter displays only a white area, and the masking is more by feel. This often introduces blurred fragments into dark iris images.

- **High Pass filter:** On the other hand, this filter is more suitable for dark irises, but can even handle light irises very well. It is the most successful of the filters because the High Pass etches the entire iris and highlights the most focused parts of the image. Therefore, there is no need to have as much contrast in the iris as in the previous approach. Applying this filter transforms the image to a grey colour where edges are generally easier to see. The sharper the edge, the better it is to see, because of this, there is less bad masking or introduction of blurred fragments into the image. As a result, excessive contrast on light irises can cause some blurred edges to appear focused on the filter

- **Edge detection + High Pass filter:** A combination of these two methods is the least useful. This is mainly because the sharp fragments from one filter are combined with the blurred fragments of the other method. This leads to overlapping and creating a degree of uncertainty as to whether the fragment is focused or not. This results in a high incidence of blurred or low-focused fragments in the resulting image. The combination of these is quite ineffective because you have to create two masks even though one of the masks contains all the needed focused fragments. So applying the second mask does not provide any new information, but the new mask may contain degradation elements.

Stack folder	Base	High	Edge	Both
be20z_left_stack	326.994	104.864	107.532	107.193
be20z_right_stack	322.684	98.079	97.884	97.444
be29z_left_stack	378.027	113.842	112.326	112.218
be29z_right_stack	379.089	109.955	107.855	109.981
bj21m_left_stack	524.103	82.034	82.393	81.569
bm22m_left_stack	389.27	119.136	118.746	118.738
bm22m_right_stack	392.774	119.292	120.853	119.754
cd20m_left_stack	346.97	82.387	81.778	81.912
cd20m_right_stack	340.865	84.22	84.992	84.334
dv27z_left_stack	325.299	102.983	101.53	100.847
dv27z_right_stack	332.87	107.446	105.77	105.844
fv23z_left_stack	292.23	58.814	59.553	59.057
fv23z_right_stack	273.324	57.988	56.753	56.794
hl23m_left_stack	430.803	113.223	113.344	112.41
hl23m_right_stack	397.235	110.833	108.497	108.271
ho33m_right_stack	418.247	118.137	117.017	117.846
kj21m_left_stack	492.636	116.785	116.339	114.572
kj21m_right_stack	381.686	125.958	124.707	123.596
km20z_left_stack	383.325	106.803	104.764	105.033
km20z_right_stack	370.753	97.848	98.941	97.798
mm18m_left_stack	299.061	92.134	91.292	90.66
mm18m_right_stack	306.937	90.931	90.541	90.064
mv21z_left_stack	401.873	96.204	96.099	96.466
mv21z_right_stack	399.111	96.258	96.386	95.223
pm27m_left_stack	110.255	110.004	107.276	107.121
pm27m_right_stack_ap	497.365	135.591	134.73	133.327
pm27m_right_stack_ff	409.653	119.894	119.553	119.586
pp27z_left_stack	502.458	108.221	107.048	106.407
pp27z_right_stack	517.468	125.661	127.757	126.823
ra20m_left_stack	368.428	114.963	112.882	112.7
ra20m_right_stack	393.917	109.85	110.986	110.909
sa20z_left_stack	370.072	88.727	87.776	87.306
sa20z_right_stack	384.335	94.488	95.662	93.674
si20m_left_stack	345.391	83.609	83.143	83.038
si20m_right_stack	347.915	84.749	85.311	83.887
sj24m_left_stack	354.873	102.981	100.976	100.646
ss20z_left_stack	372.255	74.38	74.93	75.28
tm26m_left_stack	457.438	107.713	107.774	106.849
tm26m_right_stack	443.018	109.186	110.164	108.731
va21z_left_stack	373.2	104.507	103.313	103.216
va21z_right_stack	374.514	107.705	107.261	107.391
vd22m_left_stack	398.454	94.159	94.828	94.288
vd22m_right_stack	401.959	96.737	95.984	95.831
vj17m_left_stack	293.148	75.242	75.598	75.118
vj17m_right_stack	387.042	75.075	74.977	74.085
vn23z_left_stack	382.781	113.219	113.871	112.345
vn23z_right_stack	388.51	113.357	111.955	112.863
zt19m_left_stack	414.207	110.89	111.396	111.508
zt19m_right_stack	470.463	107.56	106.682	106.248
zv23m_left_stack	387.265	95.823	96.025	95.185

Table 7.1: Table of individual image results

7.3.2 Automatic method

As has already been mentioned earlier, the method shows a high error rate when identifying the iris, when the circle-locating algorithm incorrectly marks and identifies the iris in an image. There are two main reasons for this that are related to the shape of the iris. First, the iris does not always show elements of a circular shape, and in some pictures, due to deformation, it is more like an ellipse. Second, the eyelids sometimes reaching into the shape of the iris. When applying filters and thresholds, these two formations merge into one and the algorithm then finds it hard to recognize a circle. A possible solution here is to use a neural network as a classifier of the iris and pupil, or a possible combination of functions to search the circle and ellipses in the image. However, setting individual values in matrices and thresholds is too general to prevent false-positive iris and pupil detection. In addition, such an adjustment should be varied based on the colour of the iris and the illumination intensity of the individual image. These two factors play the biggest role in the subsequent edge detection and applied threshold in a given image. Some of the measures for better results have already been implemented in the algorithm. They have significantly contributed to improving the results. Since the output of this method is bitmaps, it is not possible to make a reasonable comparison of individual sets even with the manual method.

7.3.3 Imaging method

The proposed methodology also has some very good results with a corresponding image database. After a later analysis of the resulting images and user questionnaires, suggestions for improvement arose. First, the user experience, more precisely, comfort when being scanned and its speed. Then, some alterations of a technical nature in the scanning methodology. These include, for example, improved scanning in terms of using multiple sensors or an autofocusing system. The basic criteria have been fulfilled and can be summarized as follows:

- **Quality of the depth maps:** Thanks to the high resolution images, the depth maps very detailed and contain a high degree of information. At maximum zoom, some of the marker microscopic structures can be seen to not have sufficient detail drawing. This is due to the physical limits of the lens and to get an even more detailed structure a macro converter lens or magnifying rings would be needed.
- **Stress factor:** According to respondents who have experience with other ophthalmic devices, the stressed factor was several times lower than with other devices. However, they suffered from a relatively long exposure to the light source. The problem occurred in people, whose optic systems or optic nerves were sensitive to greater light intensity. Even at the lowest possible light source, they tend to close their eyes or turn their eyes away from the light source. One solution is to increase the diffusion layer at the light source, without using the guide tunnel from the lens. This will ensure that there is no space for dispersion and the full intensity will be directed to the iris. As a result, it will be possible to significantly reduce the emitted light intensity, which will not be disperse to the environment.

- **Imaging process:** the whole process of imaging one eye takes about 5 minutes. All the time, the eye is exposed to a source of light, which for some was not pleasant. There are several reasons why the process takes so long. There is the need to localize the eye, done in such a way that the camera is set to a suitable position, also taking in the sides and height of the subject being imaged. The lens had to be set to the desired distance in order to focus on different planes. With each new focusing, it was necessary to position the iris so as to have it as much on the same plane as the previous image as possible. Using the head rest as needed to see into the fundus camera 7.2 would speed up the process considerably. With the lens set to the desired distance, special sliding rails can be used to position the camera corpus. The rails will then provide a faster and more accurate setting of the required minimum distance and stillness of the camera after finding the appropriate position. Another factor that contributed negatively to increasing the total imaging time was making multiple versions of the images, for instance, with different aperture sizes.

Certain recurrent patterns seen during imaging lead to the creation of theses that would be worth investigating on a larger statistical sample to see, if it was just a statistical error or a mistake in the methodology. These theses will also be consulted with ophthalmologists and any resulting findings will be incorporated into the methodology.

- **Eye defects:** One of the thesis talks about possible manifestations of eye defects in healthy, imaged subjects. This is based on the fact that during imaging, a healthy subject focuses on the centre of the lens. As a result, the pupil is also directed toward the centre and thus the light source is accurately projected into it. For some, however, there was a phenomenon that, when focused on the centre of the lens, the pupil was outside the centre and the light source reflected in the iris structure. If the subject focused in the opposite direction to the pupil, it was centred and the light source reflected correctly. As shown in Figure 7.5, the right image of the lens focuses on the centre of the lens, and in the left image there is then correction and the imaged subject then focused on the right corner of the lens. Similar behaviour was seen in subjects diagnosed with *Amblyopia*.

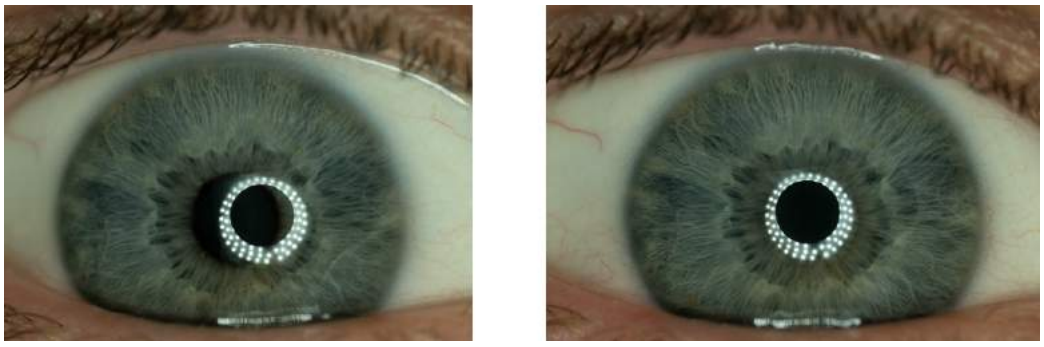

Figure 7.5: Possible hint of Amblyopia. *Right*: eye focusing on the centre of the lens, *Left*: eye after focus correction at the edge of the lens.

Another side issue of imaging is the veins found in the sclera. The notes illustrated by picture 7.6, where, in the first picture can be seen an eye that has not been exposed to any physical stress during the day. In the second picture, there is an eye that has been exposed to normal physical stress, i.e. sitting at a monitor or other aggressive light sources. The last picture shows an eye that has been exposed to extreme stress and damage in the form of intensive, persistent radiation. It is therefore provable that the veins of the eye too are variable. This significantly reduces their identification ability.

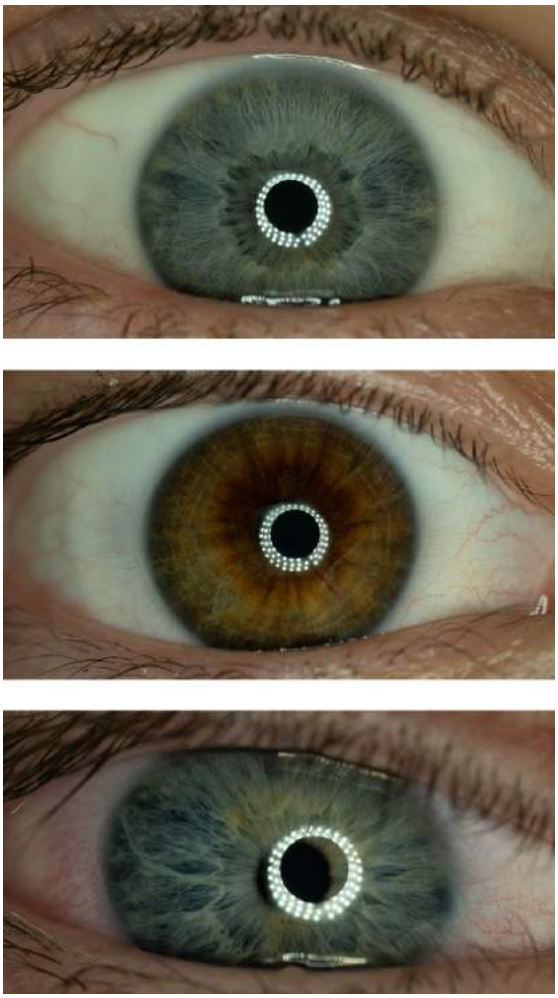

Figure 7.6: Veins in the sclera. *Top*: Eye without physical stress, *Middle*: Eye exposed to normal physical stress, *Bottom*: Eye exposed to extreme physical stress.

After analysing the images taken and applying some post-production adjustments, it became clear that it is better to have the image slightly overexposed to achieve better visible details in dark eyes, especially pure brown. If necessary, during imaging, increase the intensity of brightness in such irises.

Chapter 8

Conclusion

Thanks to the theoretical foundations mentioned in 4, 5.2 and based on the experimental images made it was possible to lay the foundations for the methodology. The methodology itself has been changed several times mainly due to changes in the technology used. Because of these changes, it was necessary to significantly modify and, in particular, reconsider some of the conclusions that emerged from experimental testing. Real-time scanning showed some shortcomings in the methodology, but these were soon reworked and a new iteration was created without the need to change the existing methodology significantly. The methodology then gradually, despite several iterations, crystallized into its current form, when it was possible to create an iris database with precise specifications according to this methodology.

Two approaches were chosen to investigate methods for iris image macro stacking and to create subsequent depth maps. One manual and the other automatic. In the first-mentioned, 3 methods were examined. High pass filter, Edge detection and a combination of both. Testing the methods subsequently showed that High Pass was the most successful method and, in contrast, the combination of methods was a complete disappointment. In general, the manual method can be said to be accurate in identifying the iris, since the human factor plays a significant role here. We are capable of determining the position of the iris very precisely. Stacking methods, however, gave rather average results, mainly due to micro eye movements between images. The automatic method then showed a higher error rate in the identification of the iris and pupil, and the images had to be largely normalized and transformed. However, the bitmaps generated by this method proved to be of very good quality. The fact that both methods returned average results led to the greatest change in the proposed methodology.

Experimentally, several images were created using filter variations, which could be used in the future in multimodal biometric systems, where they will be used primarily for further research and development of scanning methods and human iris processing in high resolution. Analysis of the questionnaires that were given to subjects immediately after scanning together with the comparison of already existing solutions, led to improved scanning designs so that it would be as user-friendly as possible and not expose the subject to unnecessary stress. Answers from the questionnaires also suggested that the requirement to reduce the stress factor affecting the eye was met. Finally, the information from the questionnaires will also serve as additional data for medical analysis. Thanks to the high resolution of the resulting photos, it will be possible to better diagnose various vision disorders. Some of them became apparent during the actual scanning.

The resulting iris database can be divided into two sections. One that contains high-resolution irises scanned using the described methodology. These images will then serve mainly for ophthalmologic and biometric purposes, where they will help to develop new technologies and knowledge. The second section contains data and outputs from macro stacking methods, which serve to show in which direction iris-sensing technology could go in the future.

Bibliography

[1] Barolet, D.: *Infrared does more good than bad for the skin: how can we learn from the sun.* [Online; visited 14.01.2018].
Retrieved from: https://atlasofscience.org/infrared-does-more-good-than-bad-for-the-skin-how-can-we-learn-from-the-sun/

[2] Bradley, J. C.; Bentley, K. C.; Mughal, A. I.; et al.: The Effect of Gender and Iris Color on the Dark-Adapted Pupil Diameter. *Journal of ocular pharmacology and therapeutics.* vol. 2010, no. 4. 2010: pp. 335 – 340. doi:10.1089/jop.2010.0061.

[3] Burge, M. J.; Bowyer, K. W.: *Handbook of Iris Recognitions.* Springer. 2006-10-31. ISBN 978-1447144014.

[4] Dobeš, M.; Machala, L.: *Digital Non-Mydriatic Retinal Cameras - CR2.* [Online; visited 07.05.2019].
Retrieved from: http://phoenix.inf.upol.cz/iris/

[5] Fleming, D.: *Depth of Field Equations.* [Online; visited 04.05.2019].
Retrieved from: http://www.dofmaster.com/equations.html

[6] Gong, Y.; Zhang, D.; Shi, P.; et al.: High-Speed Multispectral Iris Capture System Desing. *IEEE Transactions on instrumentation and measurement.* vol. 2012, no. 4. 2012: pp. 1966 – 1978.

[7] Heiting, G.: *Pupil: Aperture Of The Eye.* [Online; visited 09.01.2018].
Retrieved from: http://www.allaboutvision.com/resources/pupil.htm

[8] Heiting, G.: *Sclera: The White Of The Eye.* [Online; visited 10.01.2018].
Retrieved from: http://www.allaboutvision.com/resources/sclera.htm

[9] in The Chinese University of Hong Kong, C. V. L.: *CUHK Iris Image Dataset.* [Online; visited 07.05.2019].
Retrieved from: http://www.mae.cuhk.edu.hk/~cvl/main_database.htm

[10] How, K.: *Genialer Spickzettel für Fotografen als kostenloser Download.* [Online; visited 01.05.2019].
Retrieved from: http://blog.hamburger-fotospots.de/genialer-spickzettel-fuer-fotografen-als-kostenloser-download/

[11] Hull, C.: *What Is ISO and How to Use It in 4 Simple Steps.* [Online; visited 30.05.2019].
Retrieved from:
https://expertphotography.com/understand-iso-4-simple-steps/

[12] Kolb, H.: *Webvision: The Organization of the Retina and Visual System*. [Online; navštíveno 14.01.2018].
Retrieved from: http://webvision.med.utah.edu

[13] Kumar, A.: *DSLR Photography 101: What is ISO?* [Online; visited 07.05.2019].
Retrieved from:
https://www4.comp.polyu.edu.hk/~csajaykr/IITD/Database_Iris.htm

[14] ledsviti.cz: *LEDsviti.cz: Stupeň krytí*. [Online; visited 17.04.2019].
Retrieved from: https://www.ledsviti.cz/stupen-kryti/

[15] Lukeš, M.: *Makrofotografie a poměr zvětšení*. [Online; visited 25.05.2019].
Retrieved from: https://www.megapixel.cz/makro-fotografie-a-pomer-zvetseni

[16] Mansutov, N.: *What is Crop Factor?* [Online; visited 25.05.2019].
Retrieved from: https://photographylife.com/what-is-crop-factor

[17] Marom, E.: *Macro photography: Understanding magnification*. [Online; visited 19.04.2019].
Retrieved from: https://www.dpreview.com/articles/6519974919/macro-photography-understanding-magnification

[18] Morris, P. J.: *How are human eye colors inherited?* [Online; visited 14.01.2018].
Retrieved from: http://www.athro.com/evo/gen/inherit1.html

[19] Nischler, C.; a další, R. M.: Iris color and visual functions. *Graefes Arch Clin Exp Ophthalmol*. vol. 2013, no. 251. 2012-04-12: page 195–202.
doi:10.1007/s00417-012-2006-8.

[20] O'Neill, M.: *DSLR Photography 101: What is ISO?* [Online; visited 01.05.2019].
Retrieved from: https://animoto.com/blog/personal/dslr-photography-iso/

[21] Oyster, C. W.: *The Human Eye: Structure and Function*. Sinauer Associates is an imprint of Oxford University Press. 2006-02-06. ISBN 978-0878936441.

[22] Pihan, R.: *Ostření a hloubka ostrosti - 2. hloubka ostrosti*. [Online; visited 04.05.2019].
Retrieved from: http://www.fotoroman.cz/tech2/focus2.htm

[23] Proencça, H.: Ris Recognition: On the Segmentation of Degraded Images Acquired in the Visible Wavelength. *IEEE TRANSACTIONS ON PATTERN ANALYSIS AND MACHINE INTELLIGENCE*. vol. 2010, no. 8. 2010: pp. 1502 – 1516.
doi:10.1109/TPAMI.2009.140.

[24] Rozsíval, P.: *Oční lékařství*. Galén. 2017-08. ISBN 978-8074923166.

[25] Seebe, F.: Light Sources and Laser Safety. *Fundamentals of Photonics*. vol. 2010. 2008: pp. 39 – 72. doi:10.1117/3.784938.ch2.

[26] Serge, L.: *Eye Anatomy: Parts Of The Eye*. [Online; visited 10.01.2018].
Retrieved from: http://www.allaboutvision.com/resources/anatomy.htm

[27] Synek, S.; Šárka Skorkovská: *Fyziologie oka a vidění 2., doplněné a přepracované vydání*. Grada. 2006-10-31. ISBN 978-8024739922.

[28] Tirosh, U.: *DIY wax-fen flash diffuser - Yet another bouncy thingy.* [Online; visited 17.04.2019].
Retrieved from: https://www.diyphotography.net/diy-wax-fen-flash-diffuser/

[29] U.S.A, C.: *IIT Delhi Iris Database (Version 1.0).* [Online; visited 10.05.2019].
Retrieved from: https://www.usa.canon.com/internet/portal/us/home/products/details/eyecare/digital-non-mydriatic-retinal-cameras/cr-2

[30] Youssef, P. N.; Sheibani, N.; Albert, D. M.: Retinal light toxicity. *IEEE TRANSACTIONS ON PATTERN ANALYSIS AND MACHINE INTELLIGENCE.* vol. 25, no. 1. 2010: pp. 1 – 14. doi:10.1038/eye.2010.149.

[31] Zaborowski, R.: *Barevná teplota.* [Online; visited 14.01.2018].
Retrieved from: http://www.techniled.cz/20-barevna-teplota/

[32] Čihák, R.: *Anatomie 3.* Grada. 2016-01-22. ISBN 978-8024756363.

[33] Švábová, V.: *Barva očí brněnských vysokoškoláků. 2012.*

Appendix A

CD Content

db/: Databases of irises,

scripts/: Scripts for automatic and manual iri stacking methods,

tex/: LaTeX source of this document,

readme.txt: About how to databases and script use,

xkubic34-dip.pdf: PDF file of this document.